FORMULATION OF SUBGRID VARIABILITY AND BOUNDARY-LAYER CLOUD COVER IN LARGE-SCALE MODELS

M. EK, L. MAHRT, S. CHANG, G. LEVY, AND A. A. M. HOLTSLAG

COLLEGE OF OCEANIC AND ATMOSPHERIC SCIENCES
OREGON STATE UNIVERSITY
CORVALLIS, OREGON 97331-2209 USA

FINAL REPORT, AFOSR GRANT NO. F49620-9610058
1 MARCH 1996 - 28 FEBRUARY 1999

PREPARED FOR:

AIR FORCE OFFICE OF SCIENTIFIC RESEARCH (AFOSR/NM)
ATMOSPHERIC SCIENCE PROGRAM
DEPARTMENT OF THE AIR FORCE
801 N RANDOLPH STREET, RM 732
ARLINGTON, VA 22203-1977 USA

DISTRIBUTION STATEMENT A
Approved for public release;
Distribution Unlimited

19990302034

DTIC QUALITY INSPECTED 1

Contents

Chapter 1. Introduction

Chapter 2. A two-source canopy model with two-scale subcanopy mixing (Ek and Mahrt)

Chapter 3. Interactions of the land-surface with the atmospheric boundary layer at Cabauw (Ek and Holtslag)

Chapter 4. The simulated response of the marine atmospheric boundary layer in the western Pacific warm pool region to surface flux forcing (Levy and Ek)

Chapter 5. A boundary-layer cloud cover formulation based on a top-hat moisture distribution (Ek)

Chapter 6. Summary of PILPS studies

Chapter 7. Concluding remarks

Articles prepared under this contract

Appendix. Oregon State University atmospheric boundary layer model user list

REPORT DOCUMENTATION PAGE

AFRL-SR-BL-TR-99-

0060

Public reporting burden for this collection of information is estimated to average 1 hour per response, inc gathering and maintaining the data needed, and completing and reviewing the collection of information. collection of information, including suggestions for reducing this burden, to Washington Headquarters Se Davis Highway, Suite 1204, Arlington, VA 22202-4302, and to the Office of Management and Budget, Pape

ources, of this fferson

1. AGENCY USE ONLY (Leave blank)	2. REPORT DATE	3. REPORT TYPE AND DATES COVERED
	28 February 1999	FINAL (1 MAR 96-28 FEB 99)

4. TITLE AND SUBTITLE
FORULATION OF SUBGRID VARIABILITY AND BOUNDARY_LAYER CLOUD COVER IN LARGE-SCALE MODELS

5. FUNDING NUMBERS
AFOSR GRANT NO. F49620-9610058

6. AUTHOR(S)
M. EK, L. MAHRT, S. CHANG, G. LEVY, AND A. A. M. HOLTSLAG

7. PERFORMING ORGANIZATION NAME(S) AND ADDRESS(ES)
COLLEGE OF OCEANIC AND ATMOSPHERIC SCIENCES
OREGON STATE UNIVERSITY
CORVALLIS, OREGON 97331-2209 USA

8. PERFORMING ORGANIZATION REPORT NUMBER
NONE

9. SPONSORING/MONITORING AGENCY NAME(S) AND ADDRESS(ES)
ATMOSPHERIC SCIENCE PROGRAM
DEPARTMENT OF THE AIR FORCE
801 N RANDOLPH STREET, RM 732, ARLINGTON, VA 22203-1977 USA

10. SPONSORING/MONITORING AGENCY REPORT NUMBER

11. SUPPLEMENTARY NOTES

12a. DISTRIBUTION/AVAILABILITY STATEMENT
UNLIMITED; AVAILABLE TO PUBLIC

12b. DISTRIBUTION CODE

13. ABSTRACT *(Maximum 200 words)*

This report describes work on the Oregon State University (OSU) atmospheric boundary-layer (ABL) model under AFOSR Grant NO. F49620-9610058. This model was developed to provide ABL and land-surface parameterization schemes for large-scale numerical weather prediction models. We address five classes of model development and testing: (1) A simple two-source canopy model is proposed which accounts for canopy sparseness and turbulent mixing between the surface and canopy, and directly between the surface and air above the canopy. (2) Using updated land-surface and ABL parameterizations, a case study investigates land-surface and ABL simulations without land-surface/ABL interaction (decoupled mode), then coupled land-surface/ABL simulations where more complicated interactions and feedbacks are possible, including the formation and interaction with ABL clouds. (3) The model is used to test how different ocean surface flux forcings interact to determine marine ABL structure and development. (4) The ABL fractional cloud cover formulation is updated using a more computationally efficient top-hat distribution of specific humidity rather than the previous Gaussian distribution of relative humidity. (5) The land-surface scheme is tested using different observational data sets to assess model performance in calculating surface fluxes and soil processes.

14. SUBJECT TERMS
ATMOSPHERIC BOUNDARY-LAYER MODEL LAND-SURFACE
SURFACE FLUXES CLOUD COVER PARMETERIZATION

15. NUMBER OF PAGES
84

16. PRICE CODE

17. SECURITY CLASSIFICATION OF REPORT	18. SECURITY CLASSIFICATION OF THIS PAGE	19. SECURITY CLASSIFICATION OF ABSTRACT	20. LIMITATION OF ABSTRACT
UNCLASSIFIED	UNCLASSIFIED	UNCLASSIFIED	SAME AS REPORT

1.
Introduction

The Oregon State University (OSU) Atmospheric Boundary-Layer (ABL) model includes parameterizations of atmospheric and land-surface (and ocean-surface) physics for use in large-scale numerical weather prediction models. The research in this report addresses five classes of model development and testing: (1) sparse canopy mixing, (2) coupled land-surface/ABL modeling, (3) ocean surface fluxes and coupling with the marine ABL, (4) ABL cloud cover, and (5) land-surface modeling.

A simple two-source canopy model (Chapter 2; Ek and Mahrt) is proposed which allows for a surface with variation from bare soil to complete coverage by short vegetation, and an overlying canopy with variation from no coverage to complete coverage, and addresses the issue of canopy sparseness and subgrid variability on a scale on the order of a few kilometers or less. This increased level of sophistication allows for better comparison with the more detailed canopy observations available in many field programs which include forest canopies, rather than the single 'area-averaged' approach typical of simple land-surface schemes often used in Numerical Weather Prediction (NWP) models. While this two-source approach is not new, the partitioning of the subcanopy flux into small and large eddies (*two-scale mixing*) is new. This procedure accounts for canopy sparseness and mixing not only between the surface and canopy, but directly between the surface and air above the overlying canopy.

A case study (Chapter 3; Ek and Holtslag) investigates the interactions between the atmospheric boundary layer and the land-surface using the OSU ABL model. Simulations are made using the data set for 31 May 1978 available from the tall tower at Cabauw, Netherlands for model initialization and verification in 'off-line' simulations where the land-surface and ABL were driven separately, then in a coupled mode where more complicated interactions and feedbacks are possible, including the formation and interaction with ABL clouds. Results indicate that in coupled land-surface/ABL simulations, realistic daytime surface fluxes and atmospheric profiles are produced using the OSU ABL model with updated model parameterizations. Updated model parameterizations include a modified boundary-layer depth formulation in the ABL scheme, and changes in the soil heat flux calculation, soil hydraulic and thermal properties, and soil layering and plant root density in the land-surface scheme.

The response of marine ABL properties to surface flux forcing in the OSU ABL model is tested (Chapter 4; Levy and Ek) in a tropical convective regime using data measured during the TOGA-COARE field program. Recent experiments with NWP model flux parameterization have shown great sensitivity of the simulated large scale circulation to the heat flux parameterization in these tropical regimes but did not allow for detailed sensitivity studies of the response of the ABL integrated properties. We test how the influence of surface flux forcings affects the profiles of potential temperature and specific humidity throughout the ABL and determine its structure and depth, and the manner by which the different forcings interact with each other to determine the ABL properties.

A formulation for ABL cloud fraction within the framework of the OSU ABL model and the existing OSU ABL cloud cover formulation is presented (Chapter 5; Ek). Subgrid variability of boundary-layer moisture complicates the formulation of ABL clouds, when spatial fluctuations of moisture are large, ABL clouds first form at a lower spatially averaged humidity. A top hat distribution of moisture (specific humidity) is assumed, which in practice performs nearly as well as the more realistic Gaussian distribution, and is more computationally efficient. The formulation is based on spatially averaged specific humidity and accounts for the influences of turbulent and subgrid mesoscale variations of humidity. The turbulent variability of specific humidity near the ABL top is formulated in terms of dry air entrainment; the mesoscale subgrid variability is specified as a function of horizontal dimension (i.e. the size of a NWP grid box, e.g. 100 km).

Results of our participation in the Project for Intercomparison of Land-surface Parameterization Schemes (PILPS) are summarized (Chapter 6). The land-surface scheme from the OSU ABL model has been tested along with a number of other schemes using different observational data sets to assess model performance in the calculation of surface fluxes and soil processes.

Concluding remarks (Chapter 7) summarize findings from the current contract period, and comment on the future direction of atmospheric boundary layer modeling over land and sea, both using the OSU ABL model and in general. This is followed by a list of articles prepared under this contract. Additionally, the appendix includes a list of several recent users of the OSU ABL model at the time of this report.

2.
A two-source canopy model with two-scale subcanopy mixing

1. Introduction

We propose a simple canopy model which allows for a surface with variation from bare soil to complete coverage by short vegetation, and an overlying canopy with variation from no coverage to complete. This approach follows the approaches by Friedl (1995), Norman et al. (1995), and Shuttleworth and Wallace (1985), but additionally includes *two-scale subcanopy mixing* by accounting for 'large-eddy' mixing directly between the surface and air above the overlying canopy.

2. Canopy model

The canopy model consists of the ground surface (which is a combination of vegetation and bare soil), the overlying canopy vegetation surface, and the air in the canopy (Figure 1). Initially we allow for no heat storage in the mass of the canopy vegetation, or in the canopy air. We solve a system of equations representing energy budgets for the surface, canopy, and canopy air, which yields temperature and moisture, and turbulent fluxes for each of these three systems.

2a. surface energy budget

The energy budget at the surface is

$$S_s \downarrow + L_s \downarrow - L_s \uparrow - H_s - E_s - G = 0 \qquad (1)$$

where $S_s \downarrow$ and $L_s \downarrow$ are the incoming solar (shortwave) and downward atmospheric (longwave) radiation absorbed at the surface, respectively, $L_s \uparrow$ is the emitted surface radiation, H_s and E_s are the surface sensible and latent

heat fluxes, respectively, and G is the heat flux into the soil.

The solar radiation absorbed at the surface is

$$S_s \downarrow = S \downarrow (1 - \alpha_s)[\sigma_c t_c (1 - \alpha_c) + (1 - \sigma_c)] \tag{2}$$

where $S \downarrow$ is the clear sky incoming solar radiation, α_s is the ground surface albedo, σ_c is the overlying canopy (horizontal) fraction, t_c is the transmission ('permeability') of solar radiation through the overlying canopy, and α_c is the albedo of the overlying canopy ($0 \leq \sigma_c, t_c, \alpha_s, \alpha_c \leq 1$). Solar radiation not reflected by or absorbed in the overlying canopy is transmitted to the surface where part is absorbed. Solar radiation reflected by the surface is absorbed by or transmitted up through the canopy, with no downward reflection allowed. Canopy fraction (σ_c) and canopy transmission (t_c) are functions of solar elevation

$$\begin{aligned} \sigma_c &= \sigma_{c0} sin\phi \\ t_c &= t_{c0} sin\phi \end{aligned} \tag{3}$$

where σ_{c0} is the canopy fraction viewed from directly overhead, t_{c0} is the canopy transmission for overhead sun, and ϕ is the solar zenith angle. We assume that overhead canopy transmission is a function of vegetation density through the leaf area index (LAI), where $t_{c0} = exp(-0.5LAI)$ following Norman et al. (1995).

The downward longwave radiation at the surface is

$$L_s \downarrow = (1 - \sigma_{c0}) L \downarrow + \sigma_{c0} L_c \tag{4}$$

where $L \downarrow$ is the clear sky atmospheric radiation (above the overlying canopy), and L_c is the downward longwave radiation emitted by the overlying canopy.

The longwave radiation emitted by the surface is

$$L_s \uparrow = \epsilon_s \sigma T_s^4 \tag{5}$$

where ϵ_s is the surface emissivity, σ is the Stefan-Boltzmann constant ($5.67x10^{-8}Wm^{-2}K^{-4}$), and T_s is the surface temperature.

The surface sensible heat flux is formulated as a two-source process of the form

$$H_s = f(\sigma_c)H_{s0} + (1 - f(\sigma_c))H_{sa} \tag{6}$$

where H_{s0} is the surface sensible heat flux associated with small eddy mixing between the surface and air in the overlying canopy, and H_{sa} is the surface sensible heat flux associated with large eddy mixing between the surface and the air above the overlying canopy (the surface layer in the atmospheric boundary layer). $f(\sigma_c)$ is a function of the canopy coverage and canopy spacing, and will be discussed further below. The surface sensible heat fluxes associated with small and large eddy mixing are

$$\begin{aligned} H_{s0} &= \rho c_p g_{s0}(T_s - T_{ca}) \\ H_{sa} &= \rho c_p g_{sa}(T_s - T_a) \end{aligned} \tag{7}$$

where ρ is air density, c_p is specific heat ($1004.5Jkg^{-1}K^{-1}$), g_{s0} is the small-eddy surface (scalar) conductance, T_{ca} is the temperature of the air in the overlying canopy, g_{sa} is the large-eddy surface (scalar) conductance, and T_a is the air temperature in the atmospheric surface layer. As canopy coverage *increases*, small-eddy mixing between the surface and the canopy air increasingly dominates via the $f(\sigma_c)H_{s0}$ term in (6), while the large-eddy mixing diminishes via the $(1 - f(\sigma_c))H_{sa}$ term in (6). (As an example, $f(\sigma_c) = \sigma_c^n$, where $n = O(\geq 1)$. (In the study here, we initially chose $n = 1$.). Conversely, as the canopy coverage *decreases*, large-eddy mixing increasingly dominates over small-eddy mixing. This arrangement allows for subcanopy mixing while providing a continuous solution under a full range of canopy coverage.

The surface conductances are defined as

$$\begin{aligned} g_{s0} &= a' + b'U_s \\ g_{sa} &= f(U_a, Ri_b, \psi) \end{aligned} \tag{8}$$

following Norman et al. (1995) for the small-eddy surface (scalar) conductance, g_{s0}, where a' and b' are empirical coefficients ($0.004ms^{-1}$, and 0.012, respectively), and U_s is the wind speed above the soil surface where the effect of the soil surface roughness is minimal (typically 0.5 to 0.2 m). For the large-eddy surface (scalar) conductance, g_{sa}, we use a standard turbulent transfer coefficient, a function of the above-canopy wind speed (U_a), and the surface-to-above-canopy stability, e.g. via an explicit bulk Richardson number (Ri_b), or implicitly through an iterative solution of the ψ stability functions (Paulson, 1970). Monin-Obukhov similarity theory is not expected to be applicable to the calculation of surface exchange coefficients for sub-canopy mixing, but is applied here as it is valid in the limit of no overlying canopy.

The two-source formulation for the surface latent heat flux is

$$E_s = f(\sigma_c)E_{s0} + (1 - f(\sigma_c))E_{sa} \tag{9}$$

where E_{s0} and E_{sa} are the small and large eddy mixing latent heat flux expressions analogous to those for sensible heat flux in (6-7) defined below as

$$\begin{aligned} E_{s0} &= \rho L_v g_{s0}(q_s - q_{ca}) \\ E_{sa} &= \rho L_v g_{sa}(q_s - q_a) \end{aligned} \tag{10}$$

where L_v is latent heat ($2.5x10^6 Jkg^{-1}$), q_{ca} is the specific humidity of the air in the overlying canopy, q_s is the surface specific humidity (of the combined surface vegetation and bare soil), and q_a is the specific humidity in the atmospheric surface layer.

In order to determine q_s, we can write (10) as

$$\begin{aligned} E_{s0} &= \beta_{s0}\rho L_v g_{s0}(q_{s,sat} - q_{ca}) \\ E_{sa} &= \beta_{sa}\rho L_v g_{sa}(q_{s,sat} - q_a) \end{aligned} \tag{11}$$

where $q_{s,sat}$ is the surface saturation specific humidity, a function of T_s (e.g. using the expression by Lowe, 1977), β_{s0} and β_{sa} are the surface potential

evaporation fractions for the small and large eddy latent heat fluxes, respectively. (The potential evaporation fraction is the ratio of actual evaporation to the potential evaporation and accounts for the reduction in actual evaporation from potential evaporation due to the stomatal control by plants.) Using (9) - (11) we then determine q_s

$$\begin{aligned} q_s &= q_{ca} + \beta_{s0}(q_{s,sat} - q_{ca}) \\ &= q_a + \beta_{sa}(q_{s,sat} - q_a) \end{aligned} \tag{12}$$

Instead of potential evaporation fraction (β_{s0},β_{sa}), (11) may be also written in terms of the moisture conductance which is a more common expression to describe the stomatal control of plants

$$\begin{aligned} E_{s0} &= \frac{\rho L_v g_{s0}(q_{s,sat} - q_{ca})}{(1 + g_{s0}/g_{sm})} \\ E_{sa} &= \frac{\rho L_v g_{sa}(q_{s,sat} - q_a)}{(1 + g_{sa}/g_{sm})} \end{aligned} \tag{13}$$

where g_{sm} is the surface moisture conductance. The potential evaporation fractions can then be related to surface moisture conductance by equating (11) and (13)

$$\begin{aligned} \beta_{s0} &= \frac{g_{sm}}{g_{sm} + g_{s0}} \\ \beta_{sa} &= \frac{g_{sm}}{g_{sm} + g_{sa}} \end{aligned} \tag{14}$$

We adopt the traditional 'Stewart-Jarvis' approach and model the moisture conductance in terms of environmental forcing variables

$$g_{sm} = g_{sm,max} f(S_s \downarrow) f_s(T) f_s(q) f_s(\Theta) \tag{15}$$

where $g_{sm,max}$ is the maximum surface moisture conductance, and $f_s(S \downarrow)$, $f_s(T)$, $f_s(q)$, $f_s(\Theta)$, are functions of incoming solar radiation, air temperature, atmospheric moisture, and soil moisture content in the root zone, respectively, all dependent on the vegetation and soil type. Additionally, the effect of bare soil evaporation is included in g_{sm}.

2b. canopy energy budget

The energy budget for the overlying canopy (with no heat storage in the canopy mass) is

$$S_c \downarrow + L \downarrow + L_s \uparrow - 2L_c - H_c - E_c = 0 \tag{16}$$

where $S_c \downarrow$ is the incoming solar radiation absorbed by the canopy, H_c is the canopy sensible heat flux, E_c is the canopy latent heat flux, and the other terms have been defined previously.

The solar radiation absorbed by the canopy is

$$S_c \downarrow = S \downarrow (1 - \alpha_c)(1 - t_c)(1 + \alpha_s t_c) \tag{17}$$

The longwave radiation emitted by the canopy (both upwards and downwards) is

$$L_c = \epsilon_c \sigma T_c^4 \tag{18}$$

where ϵ_c is the emissivity of the overlying canopy, and T_c is the canopy temperature.

The canopy sensible heat flux is

$$H_c = \rho c_p g_c (T_c - T_{ca}) \tag{19}$$

where g_c is the canopy conductance for heat, which is defined as

$$g_c = \frac{LAI}{C'}\left(\frac{U_{d+z_0}}{s}\right)^{1/2} \tag{20}$$

following Norman et al. (1995) where LAI is leaf area index, C' is a weighting coefficient set equal to $90s^{1/2}m^{-1}$, s is the leaf size, and U_{d+z_0} is the wind speed at the canopy displacement height.

The canopy latent heat flux is

$$E_c = \rho L_v g_c (q_c - q_{ca}) \tag{21}$$

where q_c is the specific humidity at the canopy surface, written as an expression analogous to (10). We write the canopy latent heat flux in terms of the potential evaporation fraction (similar to (11)

$$E_c = \beta_c \rho L_v g_c (q_{c,sat} - q_{ca}) \tag{22}$$

where β_c is the canopy potential evaporation fraction, and $q_{c,sat}$ is the canopy saturation specific humidity, a function of T_c. Using (21) - (22) we then determine q_c

$$q_c = q_{ca} + \beta_c (q_{c,sat} - q_{ca}) \tag{23}$$

Instead of canopy potential evaporation fraction (β_c), (23) may be also written in terms of canopy moisture conductance

$$E_c = \frac{\rho L_v g_c (q_{c,sat} - q_{ca})}{(1 + g_c/g_{cm})} \tag{24}$$

which is analogous to (13), and g_{cm} is the canopy moisture conductance. The canopy potential evaporation fraction can then be related to canopy moisture conductance by equating (22) and (24)

$$\beta_c = \frac{g_{cm}}{g_{cm} + g_c} \tag{25}$$

where again we adopt the 'Stewart-Jarvis' approach for the canopy moisture conductance in terms of environmental forcing variables

$$g_{cm} = g_{cm,max} f_c(S\downarrow) f_c(T) f_c(q) f_c(\Theta) \tag{26}$$

similar to (15), where $g_{cm,max}$ is the maximum canopy moisture conductance. The canopy and surface moisture conductances differ due to differences in vegetation type through the maximum conductance values and the functions of environmental variables ($f_c(S\downarrow)$, $f_c(T)$, etc), and the fact that the effect of bare soil evaporation is included in g_{sm}.

2c. canopy air energy budget

The energy budget equations for the canopy air (assuming no heat storage) is

$$\begin{aligned} H_s + \sigma_c H_c - H_0 &= 0 \\ E_s + \sigma_c E_c - E_0 &= 0 \end{aligned} \tag{27}$$

where H_0 and E_0 are the sensible and latent heat fluxes, respectively, from the canopy air to the surface layer in the atmospheric boundary layer. The canopy air sensible and latent heat fluxes are

$$\begin{aligned} H_0 &= \rho c_p g_0 (T_{ca} - T_a) \\ E_0 &= \rho c_p g_0 (q_{ca} - q_a) \end{aligned} \tag{28}$$

where g_0 is the aerodynamic conductance using the standard turbulent transfer coefficients based on Monin-Obukhov similarity theory, e.g. via an explicit bulk Richardson number, or an iterative solution of the ψ stability functions (Paulson, 1970), defined here as

$$g_0 = f(U_a, Ri_b, \psi) \tag{29}$$

Using (7), (10), (19), (21) and (28), canopy air temperature and canopy specific humidity may be solved for

$$
\begin{aligned}
T_{ca} &= \frac{\sigma_c(g_{s0}T_s + g_cT_c) + g_0T_a + (1-\sigma_c)g_{sa}(T_s - T_a)}{\sigma_c(g_{s0} + g_c) + g_0} \\
q_{ca} &= \frac{\sigma_c(g_{s0}q_s + g_cq_c) + g_0q_a + (1-\sigma_c)g_{sa}(q_s - q_a)}{\sigma_c(g_{s0} + g_c) + g_0}
\end{aligned} \tag{30}
$$

3. BOREAS data set and model simulations

3a. BOREAS data

To test our canopy model, we use a data set from a boreal forest in southern Canada taken during the summer of 1994 as part of the BOREAS field program. The data set from the old aspen tower site in the southern study area of BOREAS includes 30-minute measurements of long and shotwave radiation, wind, temperature, and moisture above the canopy ($39m$), soil temperatures ($5cm$ depth), and above-canopy and subcanopy sensible and latent heat flux measurements ($39m$ and $5.5m$, respectively). This aspen forest has a canopy height of about $21m$ with a leaf area index of 1.6, and a fractional canopy coverage of about 0.5. The understory vegetation is witchhazel which has a height of about $1-2m$ and covers much of the ground surface, and a leaf area index of about 3.4.

3b. canopy model simulations

The model is initialized and driven by the tower measurements described above; verification is made against the observed above-canopy and subcanopy fluxes. For our preliminary simulation, we choose 20 August 1994, a cloud-free summertime day with minimal advection. (Partial cloud cover conditions cause rapidly changing incoming solar radiation that may affect the stomatal response of the aspen forest; this is currently not accounted for in our canopy conductance formulation.)

The model is integrated for a 24-hour period using observed radiation (Figure

2), and wind, temperature, and humidity (Figure 3). Modelled sensible (Figure 4) and latent (Figure 5) heat fluxes compare somewhat favorably with observations, although the modelled sensible heat flux is somewhat out of phase with the observations (overprediction in the morning and underprediction in the afternon) for both above-canopy and subcanopy fluxes; modelled nighttime fluxes are consistently underpredicted for both above-canopy and subcanopy fluxes. For the latent heat flux, the 'smoother' evolution of the modelled flux tends to fall in the middle of the more noisy observations during the day, with a slight overprediction in the early morning hours, and particularly well-predicted (near-zero) flux during nighttime hours.

Possible reasons for errors in model-predicted fluxes include the use of a constant albedo for the aspen forest; during early morning and late afternoon hours, a higher albedo is often observed over many vegetated surfaces which may decrease the amount of net radiation available for surface fluxes. The transmission of solar radiation through the canopy is sun-angle dependent, and has been accounted for in our model through (3), although this dependence may not be fully adequate. The choice for the value of n described after (7) determines the relative weight of the small versus large eddy subcanopy mixing. The choice of $n = 1$ gives an equal (linear) weight to the small and large eddy mixing contributions to the subcanopy flux (because the fractional canopy coverage is 0.5), and should be re-examined. For example, a choice of $n = 2$ would cause the large-eddy contribution to the subcanopy flux to drop off more rapidly. Finally, the traditional 'Stewart-Jarvis' approach for canopy conductance may be in question since it was not originally formulated for an aspen boreal forest.

4. Summary

We have proposed a two-source canopy model which includes flux contributions from an overlying canopy, and an understory which may consist of a combination of bare soil and short vegetation. This is a improvement over one-source canopy models which combine all vegetation and bare soil into one system, a difficulty when comparing to field observations which by nature often include some degree of canopy sparseness (inhomogeneity). Additionally, our canopy model includes two-scale subcanopy mixing which accounts for

small-eddy transport (flux) between the surface and canopy air, and large-eddy transport (flux) between the surface and air above the canopy. A preliminary simulation for a sparse canopy aspen boreal forest showed favorable results, but suggests that further modifications to the canopy model are necessary, e.g. in the treatment of radiation in the canopy, canopy conductance, and subcanopy mixing.

References

Friedl, M. A., 1995: Modeling land surface fluxes using a sparse canopy model and radiometric surface temperature measurements. *J. Geophys. Res.*, **100**, 25,435-25,446.

Lowe, P. R., 1977: An approximating polynomial for the computation of saturation vapor pressure. *J. Appl. Meteorol.*, **16**, 100-103.

Norman, J. M., W. P. Kustas, and K. S. Humes, 1995: Two-source approach for estimating soil and vegetation energy fluxes in observations of directional radiometric surface temperature. *Agric. For. Meteorol.*, **77**, 263-293.

Paulson, C. A., 1970: The mathematical representation of wind speed and tmperature profiles in the unstable atmospheric surface layer. *J. Appl. Meteorol.*, 9, 857-861.

Shuttleworth, W. J., and J. S. Wallace, 1985: Evaporation from sparse crops - an energy combination theory. *Quart. J. Roy. Meteorol. Soc.*, **111**, 839-855.

Figure legend

Figure 1. Schematic of simple canopy model showing radiation budget and heat fluxes. Surface varies from bare soil to complete coverage by short vegetation; overlying canopy varies from no coverage to complete. Note that surface turbulent heat fluxes (arrows) include contributions from 'small-eddy' and 'large-eddy' mixing. See text for details.

Figure 2. Time series for julian day 232 (20 August 1994) of 39.5-m air tempertaure, wind speed, and relative humidity at the 'Old Aspen' site in BOREAS used

as forcing for two-source canopy simulations.

Figure 3. As in Figure 2, but for incoming solar and downward longwave radiation.

Figure 4. Simulated sensible heat fluxes for julian day 232 (20 August 1994) at canopy-top (compared to 39.5-m observations), and at the surface (compared to 5.85-m observations) at the 'Old Aspen' site in BOREAS.

Figure 5. As in Figure 4, but for latent heat flux.

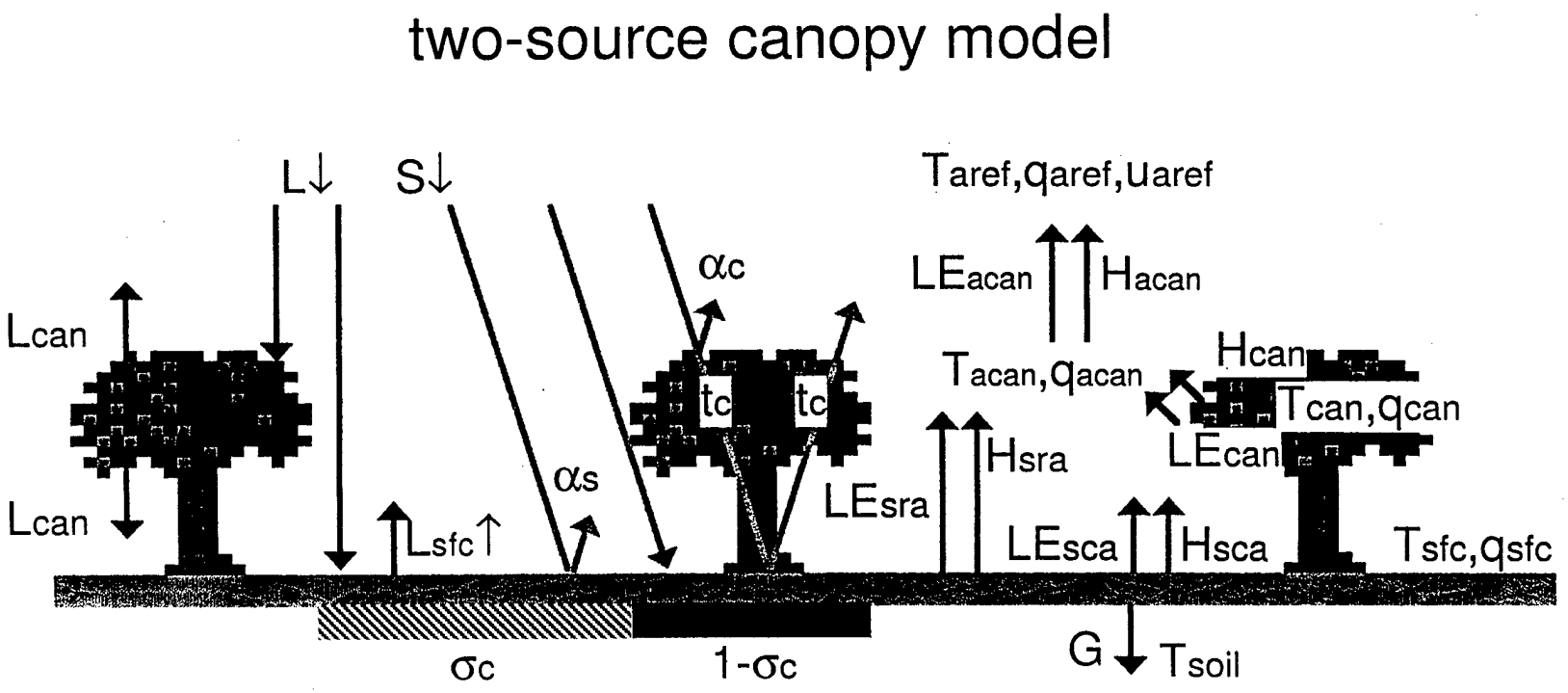
two-source canopy model
L↓
S↓
Taref,qaref,uaref
αc
LEacan
Hacan
Lcan
Hcan
Tacan,qacan
tc
tc
Tcan,qcan
Hsra
LEcan
αs
LEsra
Lcan
Lsfc↑
LEsca
Hsca
Tsfc,qsfc
G
Tsoil
σc
1-σc

Figure 1

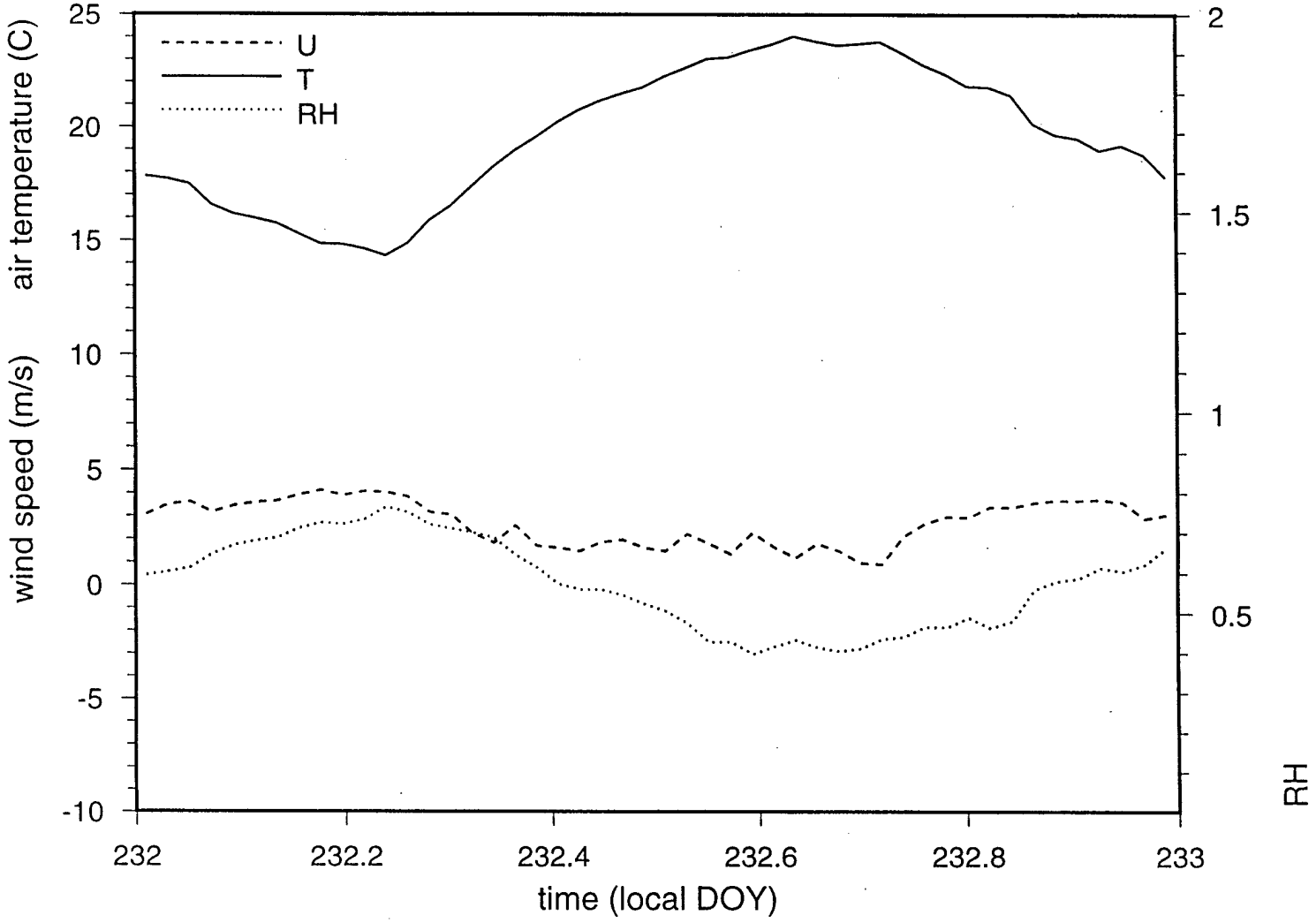
U
T
RH
wind speed (m/s)
air temperature (C)
RH
time (local DOY)
25
20
15
10
5
0
-5
-10
2
1.5
1
0.5
232
232.2
232.4
232.6
232.8
233

Figure 2

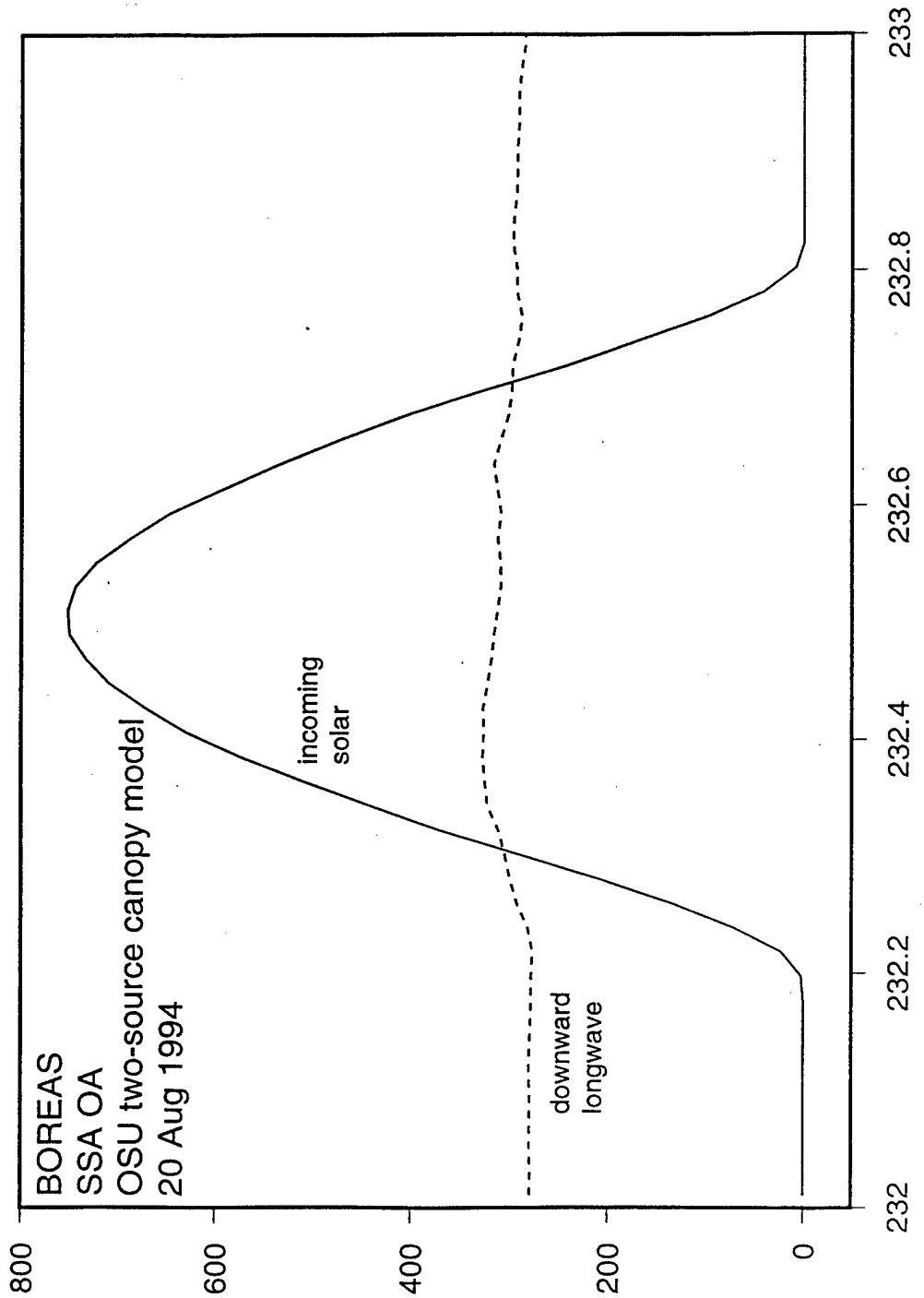
BOREAS
SSA OA
OSU two-source canopy model
20 Aug 1994
incoming
solar
downward
longwave
radiation (W/m2)
800
600
400
200
0
232
232.2
232.4
232.6
232.8
233
DOY (local time)

Figure 3

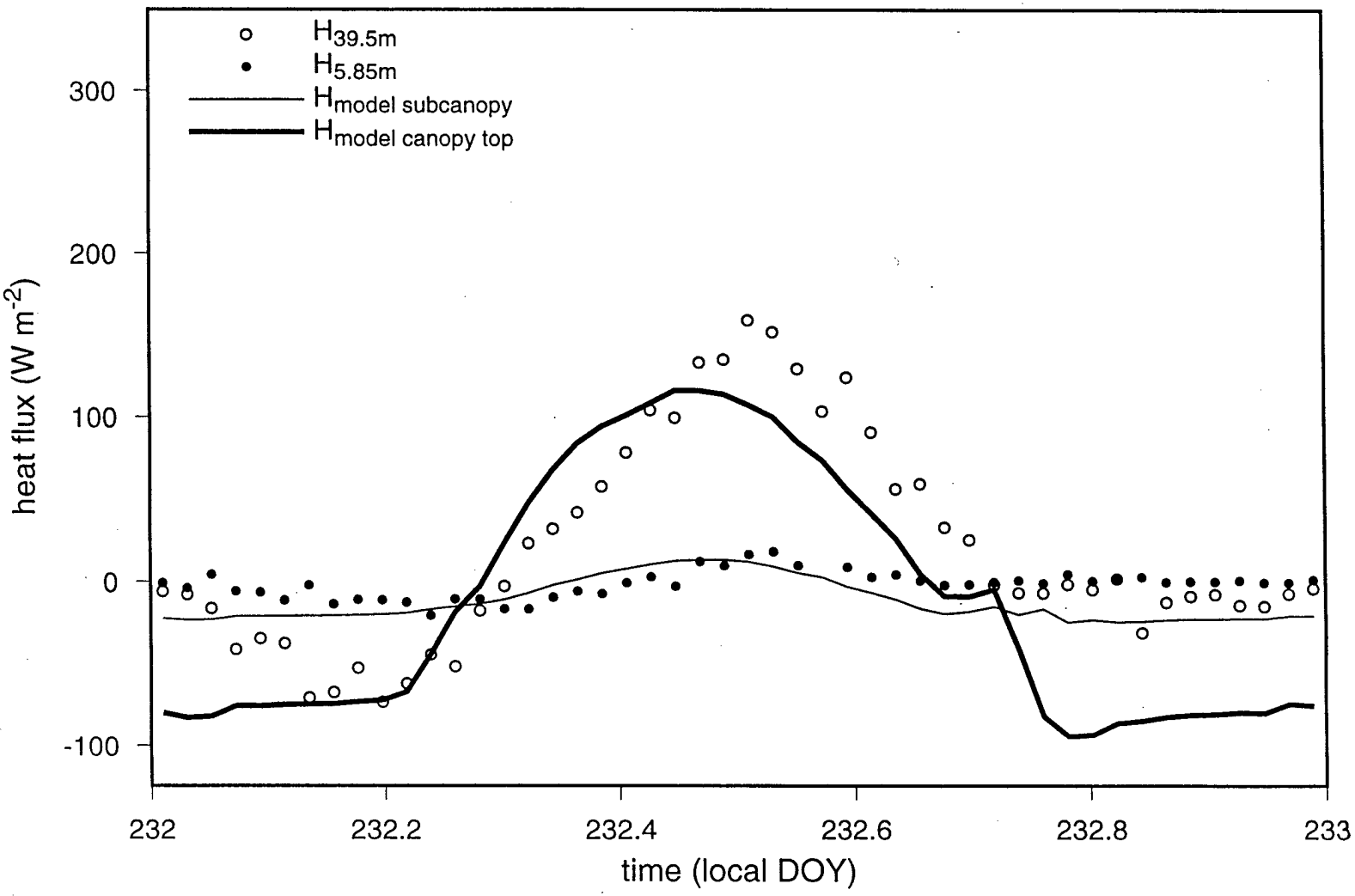
$H_{39.5m}$
$H_{5.85m}$
$H_{model\ subcanopy}$
$H_{model\ canopy\ top}$
300
200
100
0
-100
heat flux (W m^{-2})
232
232.2
232.4
232.6
232.8
233
time (local DOY)

Figure 4

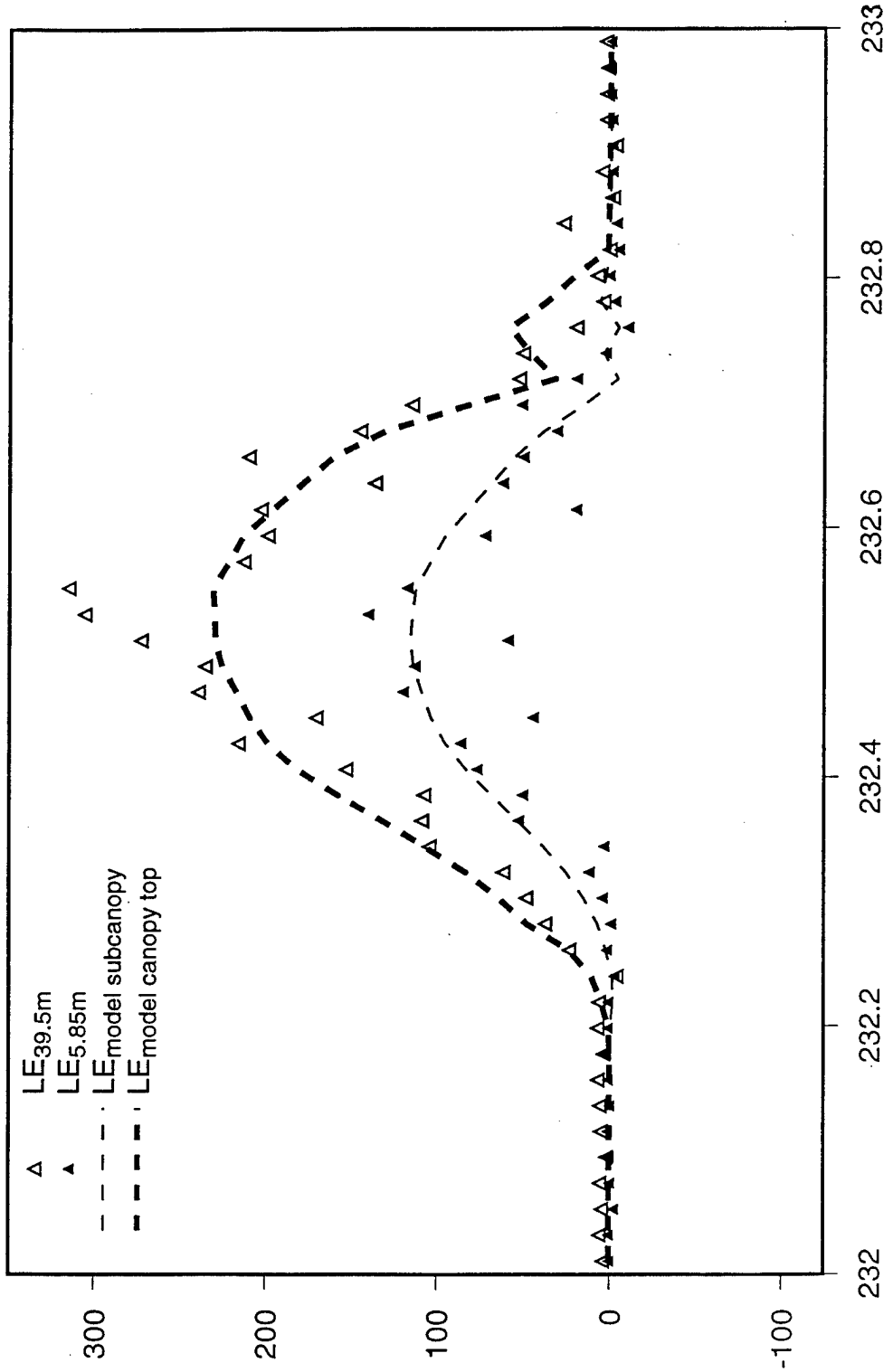
LE39.5m
LE5.85m
LEmodel subcanopy
LEmodel canopy top
heat flux (W m-2)
300
200
100
0
-100
232
232.2
232.4
232.6
232.8
233
time (local DOY)

Figure 5

3.
Interactions of the land-surface with the atmospheric boundary layer at Cabauw

1. INTRODUCTION

Recent developments in Numerical Weather Prediction (NWP) models have focused increased attention on simulation of land-surface (LS) processes (e.g. Viterbo and Beljaars, 1995 and references therein). Many of these developments have been pursued in an effort to bring the simulation of LS processes within NWP models in line with developments in the plant and soil physics communities, thereby recognizing progress in these associated disciplines. For example, Ek and Cuenca (1994) and Cuenca et al. (1996) examined the response of the atmospheric boundary layer (ABL) to soil hydraulic properties; Peters-Lidard et al. (1997; 1998) examined the effect of vegetation and soil thermal properties on soil heat flux; and Beljaars and Bosveld (1997) examined the influence of evaporative control on surface moisture flux by the vegetation at Cabauw.

The case study by Holtslag et al. (1995) examined ABL simulations driven by surface fluxes, and reproduced the observed boundary-layer structure for a case study at Cabauw. But in coupled LS-ABL simulations they found that they could not reproduce observed fluxes and boundary-layer structure using a simple land surface scheme with a constant surface conductance. Here we use the same case study day as Holtslag et al. (1995), but simulate LS-ABL interactions using the Oregon State University - Coupled Atmospheric Boundary Layer - Plant - Soil (CAPS) model which includes a more sophisticated LS scheme. (Cabauw, Netherlands, is one of the sites used during the Project for Intercomparison of Land-surface Parameterization Schemes, PILPS; Henderson-Sellers et al, 1993, 1995).

2. CABAUW SITE AND DATA SET

In this study we use observations made on 31 May 1978 at or near the Cabauw site in central Netherlands which provides the necessary information for model initialization and verification. The region surrounding the Cabauw site is rather flat for a distance of at least 20 km, with many fields and scattered canals, villages, orchards and lines of trees. One of the main branches of the Rhine, the River Lek, flows about one kilometer south of the Cabauw site (approximately 45 km east of the North Sea).

The Cabauw site itself is located in an open field of short grass which extends for several hundred meters in all directions, and contains a series of shallow, narrow ditches that provide drainage for the site. Under the sod layer (3 cm) the soil consists of heavy clay down to about

0.6 m, with a nearly saturated peat layer below. Soil moisture measurements using neutron probe were taken covering the study day at three sample sites; measurements were made at 10 cm intervals down to 50 cm, and at 1 m (Wessels, 1983).

The 213 m tower at the Cabauw site includes atmospheric observations of winds and wind stress, temperature, and specific humidity at multiple levels, and sensible and latent heat fluxes determined from profile and Bowen ratio methods. Incoming solar and longwave radiation measurements were made in a field adjacent to the tower, along with low-level, surface and soil temperatures, and low-level specific humidity measurements. The downward longwave radiation is suspect, however, being anomalously low. An estimate of downward longwave radiation was made by taking the difference between the net radiation, and net solar radiation and outgoing terrestrial (longwave) radiation computed from the infrared radiometer assuming an emissivity of unity. Soil heat fluxes were measured by transducers buried at depths of 5 and 10 cm; surface soil heat flux was inferred from extrapolation of these measurements (Beljaars and Bosveld, 1997).

Four radiosondes were launched from the Cabauw site during the morning of the study day providing temperature and moisture profiles above the tower level. Additionally the data set is supplemented with information from radiosondes launched at De Bilt (about 25 km to the northeast) several times during the day providing additional measurements of wind, temperature and moisture. Because of the proximity and similarity in surface conditions, the De Bilt observations are thought to be representative for the Cabauw site, especially above the surface layer (see Holtslag et al, 1995).

3. MODEL DESCRIPTION

The CAPS model was developed to simulate interactions of the ABL, vegetation and soil. The ABL scheme in the CAPS model follows the original development by Troen and Mahrt (1986), and includes a simple cloud cover formulation (Ek and Mahrt, 1991). The atmospheric nonlocal heat and moisture mixing is updated following Holtslag and Boville (1993), with modifications to the boundary-layer height formulation by Vogelezang and Holtslag (1996).

Surface exchange coefficients (and thus surface fluxes) are calculated by iterating an implicit formula using the Monin-Obukhov functions following Paulson (1970), replacing the previous method which used an explicit dependence on the near-surface bulk Richardson number to determine surface exchange coefficients following Louis (1979) and Louis et al. (1982). This step was taken because of a limitation in the application of the Louis formulation for cases where the ratio of the momentum to heat roughness is large, as demonstrated in Holtslag and Ek (1996). See Beljaars and Holtslag (1991) for further discussion.

The ABL scheme is coupled with an active LS scheme consisting of multiple soil layers (Mahrt

and Pan, 1984), and a simple plant canopy (Pan and Mahrt, 1987) modified to include the effect of vegetation using a 'big leaf' concept following Noilhan and Planton (1989). Additionally, the parameterization of soil processes by van Genuchten (1980) is introduced into the soil component of the CAPS model as an alternative to the more traditional meteorological approach using Clapp and Hornberger (1978) and Cosby et al (1982). Cuenca et al (1996) compared the use of van Genuchten versus Clapp and Hornberger formulations in the CAPS model, and found large differences in the simulated surface fluxes and other modelled variables for intermediate soil moisture contents. This is not surprising since different soil data sets were used to construct these parameterizations. In fact, Ek and Cuenca (1994) showed that the known variability of the parameters used in the Clapp and Hornberger formulation itself showed similar differences. The primary advantage in the use of a van Genuchten (1980) formulation is that it is m.ore widely accepted in the soil physics community so that many soil data sets are evaluated in terms of this formulation, which also has a more realistic representation of the soil moisture potential curve near saturation (see Cuenca et al., 1996). The Cabauw site soils have been specifically evaluated in terms of a van Genuchten formulation.

The CAPS model was originally formulated for inclusion in large-scale models where computational efficiency is important, yet the equations used are comprehensive enough to approximate the physical processes thought to be most important (e.g. Pan, 1990; Holtslag et al., 1990). In addition, the model has been used in a stand-alone column mode for a number of sensitivity experiments under different geophysical conditions (e.g. Ek and Mahrt, 1994; Holtslag and Ek, 1996).

4. MODEL SIMULATIONS

We first examine simulations of the LS forced by observed atmospheric and radiation conditions, followed by the ABL forced by observed surface fluxes. These 'stand-alone' tests allow us to isolate processes responsible for surface fluxes (LS scheme without ABL interaction) and ABL development (ABL scheme without LS interaction) before attempting to couple the two schemes. In a coupled mode, more complicated interactions and feedbacks are possible, including the formation and presence of ABL clouds.

4.1 Land-Surface Simulations

We initialize the LS scheme using surface and soil observations and descriptions of the Cabauw site following the PILPS-related studies by Beljaars and Bosveld (1997) and Chen et al. (1997). We drive the LS scheme in the CAPS model using the observed wind, temperature and specific humidity at 20 m, and downward solar and longwave radiation at the Cabauw site at each timestep. This allows us to evaluate the model performance in properly partitioning available incoming energy into upward longwave radiation, and sensible, latent, and soil heat fluxes. Several sensitivity tests are made involving representation of canopy resistance, soil heat

transfer, and initial soil and surface conditions.

The diurnal variation of canopy conductance for the study day can be 'extracted' from the observed surface fluxes, temperature and specific humidity measurements. Using the canopy conductance parameters from the PILPS-Cabauw study (Chen et al., 1997), we found that canopy conductance was overpredicted throughout the day, leading to an overprediction of the latent heat flux, which would have a subsequent effect on ABL development. However, using the Cabauw-specific canopy conductance parameters via Beljaars and Bosveld (1997), and a commonly-accepted (by soil scientists) plant root density function (Cuenca, 1996, personal communication), predicted canopy conductance values were found to be much closer to the observed ('extracted') values. This 'commonly-accepted' root density function assumes 40% of the roots are found in the upper quarter of the root zone, 30% in the next quarter, 20% in the next quarter, and 10% in the bottom quarter of the root zone This representation is closer to a uniform root distribution with depth, in contrast to that suggested in the PILPS-Cabauw study (70% root density in the upper 10 cm; 30% in the next 90 cm), or used in the ECMWF LS scheme (one-third of the root density each in the 0-7 cm, 7-21 cm, and 21-72 cm soil layers).

Soil heat flux is normally parameterized as a function of the soil thermal conductivity (a function of soil moisture content), and the temperature gradient over a given soil depth near the surface ('bare' soil parameterization). In the presence of a vegetation layer, soil heat flux is reduced because of the lower conductivity through this vegetation layer. This has been demonstrated by Viterbo and Beljaars (1995) and van den Hurk and Beljaars (1996) in the ECMWF LS scheme. They suggest a simpler parameterization to deal with this effect where the soil heat flux is computed from an empirical constant and the soil temperature gradient near the surface. An alternative is the function by Peters-Lidard et al. (1997) where 'bare' soil heat flux is calculated, then reduced by an exponentially increasing function of leaf area index.

Use of the '40-30-20-10' root density representation, along with the ECMWF soil heat transfer parameterization, more closely simulates the observed surface fluxes. The ECMWF and PILPS-Cabauw root density representations underpredict (overpredict) the latent (sensible) heat flux because the shallower upper soil layer dries out more quickly with a higher root density, while the uniform root density behaves more similarly to the '40-30-20-10' root density representation (latent heat flux shown in Figure 1). Using the 'bare' soil representation, soil heat flux is greatly overestimated (Figure 2), which affects the sensible and latent heat fluxes. The soil heat flux predicted by the Peters-Lidard et al. (1997) formulation also overpredicts soil heat flux, though less than the 'bare' soil case; this soil heat flux prediction could possibly be improved given Cabauw-specific thermal conductivity values.

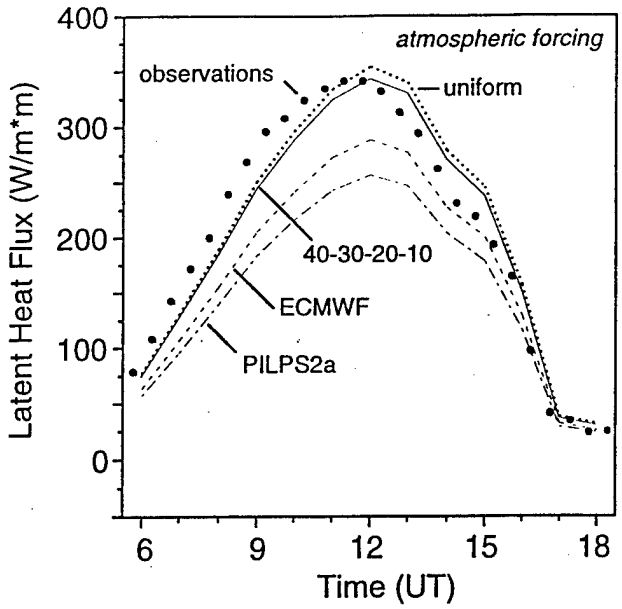

Figure 1. Cabauw, Netherlands, 31 May 1978: latent heat flux, observed (solid symbols), and predicted based on '40-30-20-10'(solid line), uniform (dotted), ECMWF (dashes), and PILPS-Cabauw (=PILPS2a, long-short dashes) root density representations.

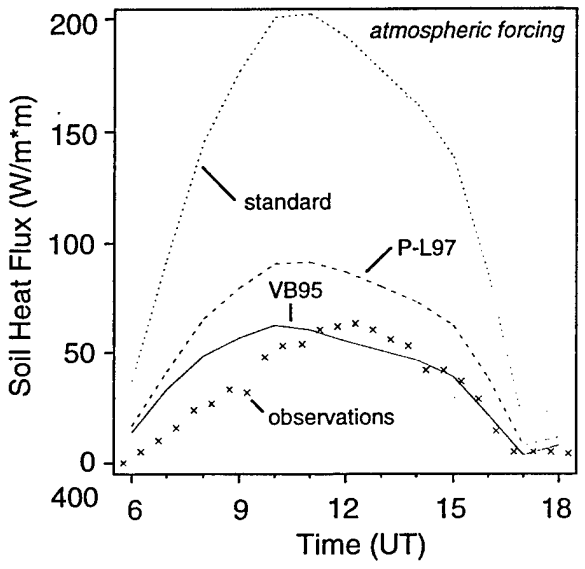

Figure 2. Cabauw, Netherlands, 31 May 1978: soil heat flux, observed ('x'), and predicted based on ECMWF (=VB95, solid line), Peters-Lidard et al., 1997 (=P-L97, dashed), and 'bare' (=standard, small dashed) soil heat flux formulations.

4.2 Atmospheric Boundary-Layer Simulations

We initialize the ABL scheme with temperature and specific humidity profiles following Holtslag et al. (1995). Because a column model often cannot adequately describe mesoscale momentum dynamics, we prescribe the winds at each timestep using Cabauw tower observations and radiosonde wind data taken during the day. By avoiding modeling of the wind, we can focus on heat and moisture mixing in the ABL, and interactions with the LS. This method was successfully used by Holtslag and Ek (1996) to deal with complicated winds and allowed them to focus on boundary-layer heat and moisture mixing and interaction with the surface.

Following Holtslag et al. (1995), large-scale subsidence and horizontal advection were thought to be minimal, so this constraint was applied to the ABL simulations here. As in Holtslag et al. (1995), temperature was found to be slightly warmer than observed in the morning hours, and about one degree cooler than observed during afternoon hours, while specific humidity is comparable to observations. Simulated ABL growth was slightly too vigorous in the morning hours, although it is better represented in the afternoon (Figure 3). When ABL clouds are 'turned-on' (but radiation still prescribed), clouds are first predicted in the mid-afternoon which is consistent with synoptic observations. (ABL clouds can be quite sensitive to horizontal and vertical advection; this topic will be explored further in future model simulations.)

4.3 Coupled Simulations

In coupled simulations, the LS and ABL are initialized as in the separate LS and ABL simulations (with observed radiation), and are allowed to operate in concert. However, it should be kept in mind that if the results from coupled simulations improve compared to results from simulations with the LS scheme alone (atmosphere/radiation forced), or with the ABL scheme alone (surface forced), then compensating errors are responsible for any improvement. It is hoped that in coupling the two schemes, the results will not be degraded. This appears to be the case in the coupled simulations for ABL development and cloud formation (Figure 3), and surface heat fluxes (Figure 4).

As an additional test, we utilize a simple radiation scheme included as an option in the CAPS model to predict downward solar (shortwave) radiation and atmospheric (longwave) radiation, and shortwave albedo at the surface. This removes an additional 'anchor' in coupled simulations, so that it is more 'fully interactive'. The ABL cloud cover predicted by the cloud cover formulation scheme then affects radiation that reaches the surface, which affects land surface processes (surface fluxes, canopy conductance, etc), and subsequent boundary-layer development, cloud cover, and so on. The ABL development and cloud formation using calculated radiation are similar to the coupled simulation using observed radiation (Figure 3), as are the surface heat fluxes (Figure 4).

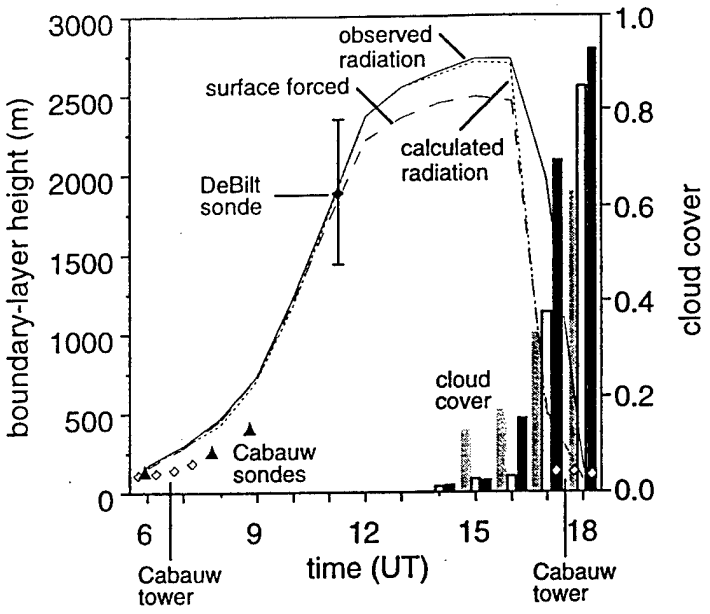

Figure 3. Cabauw, Netherlands, 31 May 1978: ABL depth from Cabauw tower observations (open diamonds), radiosonde data (solid triangles), and nearby De Bilt radiosonde data (solid diamonds; with uncertainty range); predicted ABL height and cloud cover for surface-forced ABL simulations (large dashes, gray bars), and for coupled LS-ABL simulations using observed radiation (solid line, white bars) and calculated radiation (small dashes, black bars).

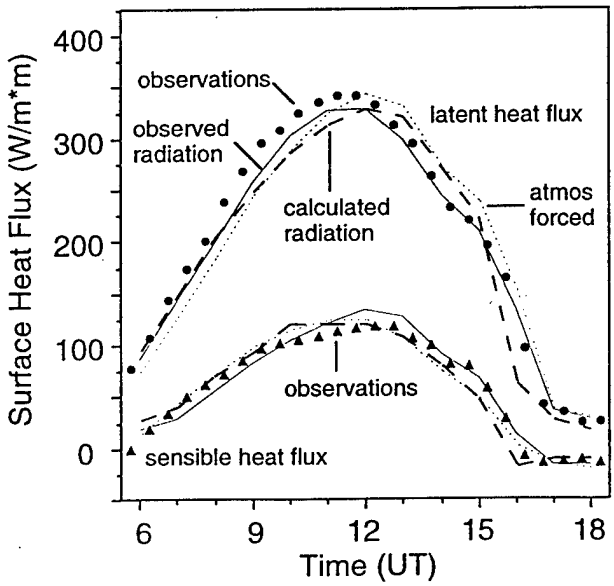

Figure 4. Cabauw, Netherlands, 31 May 1978: observed latent (as in Figure 1) and sensible (solid triangles) heat fluxes, and predicted heat fluxes based on '40-30-20-10' root density representation and ECMWF soil heat flux formulation for LS-only simulation (=atmos forced, small dashes), and for coupled LS-ABL simulations using observed radiation (solid line) and calculated radiation (large dashes).

5. SUMMARY

Results indicate that in coupled LS-ABL simulations, realistic daytime surface fluxes and atmospheric profiles including ABL clouds are produced using the CAPS model with updated model parameterizations. These updates include a modified boundary-layer depth formulation in the ABL scheme, and changes to the parameterization of soil heat flux, soil hydraulic processes, soil layering, and plant root density in the LS scheme. ABL simulations yielded encouraging results, both alone and interactively when coupled with the LS scheme. However, the affect of horizontal advection and vertical motion on the simulation of the ABL, especially when clouds form, must be more fully assessed with further study.

REFERENCES

Beljaars, A. C. M., and F. C. Bosveld, 1997: Cabauw data for the validation of land surface parameterization schemes. *J. Clim.*, **10**, 1172-1193.

Beljaars, A.C. and A. A. M. Holtslag, 1991: Flux parmeterization over land surfaces for atmospheric models. *J. Atmos. Sci.*, **30**, 327-341.

Chen, T. H., A. Henderson-Sellers, A. J. Pitman, Y. Shao, A. Beljaars, S. Chang, M. Ek, and collaborators, 1997: Cabauw experimental results for the project for intercomparison of land-surface parameterization schemes (PILPS). *J. Clim.*, **10**, 1194-1215.

Clapp, R. B. and G. M. Hornberger, 1978: Empirical equations for some soil hydraulic properties. Water Resour. Res., **14**, 601-604.

Cosby, B. J., G. M. Hornberger, R. B. Clapp, and T. R. Ginn, 1984: A statistical exploration of the relationship of soil moisture characteristics to the physical properties of soils. *Water Resour. Res.*, **20**, 682-690.

Cuenca, R. H., M. Ek, and L. Mahrt, 1996: Impact of soil water property parameterization on atmospheric boundary-layer simulation. *J. Geophys. Res.*, **101**, 7269-7277.

Ek, M. and R. H. Cuenca, 1994: Variation in soil parameters: Implications for modeling surface fluxes and atmospheric boundary-layer development. *Bound.-Layer Meteorol.*, **70**, 369-383.

Ek, M. and L. Mahrt, 1991: A formulation for boundary-layer cloud cover. *Ann. Geophysicae*, **9**, 716-724.

Ek, M. and L. Mahrt, 1994: Daytime Evolution of Relative Humidity at the Boundary-Layer Top. *Mon. Wea. Rev.*, **122**, 2709-2721.

Henderson-Sellers, A., A. J. Pitman, P. K. Love, P. Irannejad, and T. H. Chen, 1995: The Project for Intercomparison of Land-surface Parameterization Schemes (PILPS): Phases 2 & 3. *Bull. Amer. Meteor. Soc.*, **76**, 489-503..

Henderson-Sellers, A., Z.-L. Yang, and R. E. Dickinson, 1993: The Project for Intercomparison of Land-surface Parameterization Schemes (PILPS). *Bull. Amer. Meteor. Soc.*, **74**, 1335-1349.

Holtslag, A. A. M. and B. Boville, 1993: Local versus nonlocal boundary-layer diffusion in a global climate model. *J. Clim.*, **6**, 1825-1842.

Holtslag, A. A. M., E. I. F. de Bruijn, and H.-L. Pan, 1990: A high resolution air mass transformation model for short-range weather forecasting. *Mon. Wea. Rev.*, **118**, 1561-1575.

Holtslag, A. A. M., E. van Meijgaard, and W. C. de Rooy, 1995: A comparison of boundary layer diffusion schemes in unstable conditions over land. *Bound.-Layer Meteorol.*, **76**, 69-95.

Holtslag, A. A. M. and M. Ek, 1996: The simulation of surface fluxes and boundary-layer development over the pine forest in HAPEX-MOBILHY. *J. Appl. Meteorol.*, **35**, 202-213.

Louis, J.-F., 1979: A parametric model of vertical eddy fluxes in the atmosphere. *Bound.-Layer Meteorol.*, **17**, 187-202.

Louis, J.-F., M. Tiedtke and J. F. Geleyn, 1982: A short history of the operational PBL-Parameterization of ECMWF. Workshop on PBL parameterization, European Centre for Medium Range Weather Forecasts, Shinfield Park, Reading, Berks, U. K., pp. 59-79.

Mahrt, L. and H.-L. Pan, 1984: A two-layer model of soil hydrology. *Bound.-Layer Meteorol.*, **29**, 1-20.

Noilhan, J. and S. Planton, 1989: A simple parameterization of land surface processes for meteorological models. *Mon. Wea. Rev.*, **117**, 536-549.

Pan, H.-L., 1990: A simple parameterization scheme of evapotranspiration over land for the NMC medium-range forecast model. *Mon. Wea. Rev.*, **118**, 2500-2512.

Pan, H.-L. and L. Mahrt, 1987: Interaction between soil hydrology and boundary-layer development. *Bound.-Layer Meteorol.*, **38**, 185-202.

Paulson, C. A., 1970: The mathematical representation of wind speed and temperature profiles in the unstable atmospheric surface layer. *J. Appl. Meteor.*, **9**, 857-861.

Peters-Lidard, C. D., E. Blackburn, X. Liang, and E. F. Wood, 1998: The effect of soil thermal conductivity parameterization on surface energy fluxes and temperatures. *J. Atmos. Sci.*, **55**, 1209-1224.

Peters-Lidard, C. D., M. S. Zion, and E. F. Wood, 1997: A soil-vegetation-atmosphere transfer scheme for modeling spatially variable water and energy balance processes. *J. Geophys. Res.*, **102**, 4303-4324

Troen, I. and L. Mahrt, 1986: A simple model of the atmospheric boundary layer: Sensitivity to surface evaporation. *Bound.-Layer Meteorol.*, **37**, 129-148.

van den Hurk, B. J. J. M. and A. C. M. Beljaars, 1996: Impact of some simplifying assumptions in the ECMWF surface scheme. *J. Appl. Meteorol.*, **35**, 1333-1343.

van Genuchten, M. Th., 1980: A closed-form equation for predicting the hydraulic conductivity of unsaturated soils. *Soil Science Society of American Journal*, **44**, 892-898.

Viterbo, P., and A. C. M. Beljaars, 1995: An improved land surface parameterization scheme in the ECMWF model and its validation. *J. Clim.*, **8**, 2716-2748.

Vogelezang, D.H.P. and A. A. M. Holtslag, 1996: Evaluation and model impacts of alternative boundary-layer height formulations. Bound.-Layer Meteorol, **81**, 245-269.

Wessels, H. R. A., 1983: Soil moisture measurements 1977-1981 at the Cabauw micrometeorology field. Royal Netherlands Met. Inst. technical report, KNMI FM-83-19.

4.
The simulated response of the marine atmospheric boundary layer in the western Pacific warm pool region to surface flux forcing

1. Introduction

Surface and interfacial fluxes and transports have a crucial role in driving the tropical circulation but are very difficult to measure and to model. Their importance and the sensitivity of atmospheric and oceanic models to their forcing are so great however, that every effort to appraise and model their influence is of great value. The current developments in general circulation modeling (GCM) studies underscore the need for a better representation of the marine atmospheric boundary layer (MABL) processes and better understanding of model response to interfacial flux forcings. The celebrated climate drift problem is amplified in coupled GCMs due to the unrealistic surface fluxes between the atmosphere and ocean; subtle inaccuracies in the surface fluxes and boundary layer process representation change the character of the variability in the coupled atmosphere-ocean system (Gordon and Corry, 1991; Latif *et al* 1988); and small differences in surface flux were associated with a very significant increase in global sea surface temperature in GCMs (Randall *et al*, 1992). Another dramatic demonstration that underscores the sensitivity of model simulations to the MABL formulations in the tropics is presented in three recent papers: the ability of the European Center for Medium Range Weather Forecasts (ECMWF) model to simulate the entire tropical circulation was greatly enhanced because of recent, apparently minor changes in the heat flux parameterization in free convective conditions (Miller *et al* 1992; Palmer and Anderson 1994; Beljaars, 1995). Despite the very favorable impact that these changes had on the large scale simulated circulation, it is not clear that the simulated fluxes represent the actual fluxes well, thus the response of a coupled ocean model to such changes may be adverse.

The lack of high quality flux data in certain regimes (e.g., the western Pacific warm pool) has made model sensitivity tests the primary tool for evaluating parameterizations and model exchange coefficients. It has also led to

the designation of interfacial flux studies as one of the three components of the Tropical Ocean Global Atmosphere (TOGA) Coupled Ocean Atmosphere Experiment (COARE). One of the objectives of this study is to use the TOGA-COARE measured fluxes and soundings to initiate and test the Oregon State University (OSU) MABL model in the tropical convective regime. We test the response of the entire MABL to both observed fluxes and existing flux formulations. Since many GCMs employ some version of the OSU ABL model as their ABL scheme (e.g. NCEP MRF, Hong and Pan, 1996; NCAR CCM3, Hack et al, 1993), rigorous testing of this model response to the interface flux forcing is of wide interest.

The above mentioned and most other modeling studies have looked at the response of some or all of the leading processes to the transports of momentum and heat at the atmosphere-ocean interface in an integrated fashion without regard to the actual flux forcing. Stein and Alpert (1993) show that the common procedure followed in parametric (sensitivity) tests fails to separate interaction (synergistic) effects when more than one factor is involved. In this paper we apply the methodology proposed by Stein and Alpert (1993) to an ABL model in order to gain insight into the important pure and interaction effects controlled by air-sea interfacial fluxes and to critically assess parameterization schemes in the ABL model used. We achieve our objectives by a careful design of a set of numerical experiments as described in the next section. By initializing our model simulations with observed fluxes and soundings we make no prior assumptions on the flux formulation and test the model response to the perfect parameterization (contaminated only by measurement error). We then repeat our experiments with existing flux formulations.

2. Methodology and Experimental Design

2.1 Factor Separation

Numerous studies have postulated the importance of synergistic effects and non-linear interaction between factors but could not easily isolate or quantify them; many other studies have used an effect on/off sensitivity tests to

study the importance of a factor but may have in fact failed to separate pure effects. Recently Stein and Alpert (1993) have introduced a general method for separating the individual contribution of different physical (and artificial) factors in numerical simulations. In addition to separating the pure effects, this method can separate the contribution of synergistic (interaction) effects between any number of terms and processes. The method employs a series expansion and is described in full by Stein and Alpert (1993). Its application to three factors, as practiced in this paper, is summarized below.

For the full separation of three factors (momentum flux, sensible heat flux, and latent heat flux in this study) 2^3 simulations S_0, S_1, S_2, S_3, S_{12}, S_{13}, S_{23}, S_{123} are required where subscript note the effects which are turned on in each simulation (i.e., S_0 - simulation with effects 1,2, and 3 shut off; S_1 - simulation with effect 1 turned on; S_{12} - simulation with effects 1 and 2 turned on; etc.). Each simulation, S_j, yields an output field f_j. Once the simulations are complete, the pure and interaction effects are calculated from the resulting fields f_j as follows:

$$\begin{aligned}
E_1 &= f_1 - f_0 \\
E_2 &= f_2 - f_0 \\
E_3 &= f_3 - f_0 \\
E_{12} &= f_{12} - (f_1 + f_2) + f_0 \\
E_{13} &= f_{13} - (f_1 + f_3) + f_0 \\
E_{23} &= f_{23} - (f_2 + f_3) + f_0 \\
E_{123} &= f_{123} - (f_{12} + f_{23} + f_{13}) + (f_1 + f_2 + f_3) - f_0 \qquad (1)
\end{aligned}$$

where E_i, E_{ij}, E_{ijk} represent pure, dual-interaction, and triple interaction effects, respectively. As long as a factor can be identified and turned off in a simulation, there is no limit to the number of factors which can be investigated. However, the complete separation of n factors requires 2^n simulations, a liability for models with large computational requirements. Unidentified factors will be contained in the background field (f_0). The factor separation method is not convenient for investigation of the effect of a continuously

varying factor. The method does not distinguish physics from numerical and artificial effects but can be used to isolate their non-linear effects and help in evaluating parameterizations and assessing errors due to numerical problems.

2.2 Experimental Design

The unique conditions in the western Pacific warm pool region contribute to a climate regime that is very important to the tropical circulation yet had been poorly modeled in the past. Air-sea interactions in the western Pacific warm pool region are unique because of these distinctive features that include convection fueled by interfacial energy fluxes. The intensive observational period (IOP) of the TOGA-COARE program has provided us with an unprecedented set of observation for model initialization and testing in a regime that is normally poorly observed. We concentrate on a case during the IOP in typical unstably stratified conditions for which we have concurrent flux measurements and soundings taken on board the *MV Moana Wave* (e.g., Fairall *et al* 1996a,b). It is associated with a persistant low level jet though somewhat ligher winds at the surface. The simulation period was chosen based on the availability of good flux measurements (solid symbols in Figure 1) that could be used for surface-flux forced runs.

We conduct two sets of experiments, each comprised of eight simulations following the factor separation method for three factors (described above). One set is run with observed fluxes, and the other with the existing surface flux formulation (i.e., following Fairall *et al* 1996b; Beljaars, 1995). Observed fluxes are taken from the *Moana Wave* ship-board 50-minute measurements (eight observations during a 6-hr simulation beginning at 10:48 UTC) and interpolated to each model time step of the simulation (lower panels in Figures 2, 3, and 5). The existing surface flux formulation requires the sea surface temperature (SST) as forcing which is taken from the *Moana Wave*, and interpolated in the same manner as the observed fluxes. The SST values are corrected for the cool skin effect from the warm layer measurements taken by the *Moana Wave* (Fairall *et al* 1996a).

Each set of experiments is initialized with observed sounding profiles (10:48 UTC), with the temperature and moisture measurements from the lowest sounding levels (to 80 m) discarded due to reports of large errors (e.g., El-

liot and Gaffen, 1991) with the sonde wind measurements retained. *Moana Wave* ship-board observations at the surface and 15 meters are included in the initialization profile; missing temperature and moisture between 15 m and 80 m are interpolated to the observed wind levels (Figure 1).

The presence of a persistent low-level wind maximum during our simulation period (Figure 1) makes modeling the wind difficult because a stand alone column model cannot adequately describe larger (non-turbulent) scale momentum dynamics. Therefore we prescribe the eight 50-minute *Moana Wave* 15-m wind observations and the *Moana Wave* radiosonde wind profile data taken at 10:48 UTC and 16:48 UTC, interpolating for each time step. By avoiding wind modeling, we can focus on the boundary layer mixing of heat and moisture, and interactions with the ocean surface fluxes. This method was successfully employed in the study by Holtslag and Ek (1996) to deal with a complicated wind situation. Thus, the strong low level jet (Figure 2, upper four panels) and the associated differential thermal and humidity advection were prescribed as described in the next section. Runs without prescribed profile and radiation forcing (e.g. advection) were generated as part of the initialization procedure and provide another set of sensitivity tests. This additional set of experiments is identical in all initial and boundary condition except it has no prescribed advection and radiational cooling. We call these runs the zero-advection runs and use them to examine if, and to what degree the pure and interaction terms are sensitive to external (prescribed) forcings other than fluxes.

2.3 The ABL Model

The model we use for our experiments is the Oregon State University Atmospheric Boundary-Layer (OSU ABL) model, which is a one-dimensional (column) model that was developed to simulate turbulent mixing in the atmospheric boundary layer. For the marine boundary layer, a scheme to calculate ocean surface fluxes is included. The free-atmospheric diffusion scheme in the OSU ABL model is turned off so there is no vertical diffusion (turbulent mixing) above the diagnosed atmospheric boundary layer height; prescribed advection is used to account for changes above the ABL. The vertical resolution of the model is 20 meters in the lowest 80 meters of the model domain, and increases to 100 meter resolution from 200 meters to 2

km height. The lowest model level in the atmosphere is 15 meters which matches the observation level of the *Moana Wave*. The time step used in model simulations is 180 seconds, appropriate for the model (vertical) resolution. The constant horizontal advection of temperature and humidity is prescribed for each time step and varies with height; the prescribed clear-air radiative cooling is also included with the temperature advection term. These values are based on the analysis described below. The wind profile is prescribed as described above. Additional model details are given in the appendix.

3. Advection and Radiation Forcing

To make a fair comparison with observations, temperature and moisture advection and the effect of clear air radiative cooling are required for column model simulations, and must therefore be specified, as it is when such a model is coupled with a large-scale 'parent' model (e.g. a GCM). The persistent low level jet observed from the *Moana Wave* soundings (Figure 1), which is not reflected in the TOGA-COARE larger scale Intensive Flux Array (IFA) and Large Scale Array (LSA) area-averaged means (Johnson and Ciesielski, 1997) suggests that temperature and moisture advection cannot be ignored. This is supported by the changes in the temperature and moisture profiles during the 6-hr simulations. We therefore estimate the advection by balancing the total change, advection, and turbulent fluxes (and radiational cooling in the case of temperature) such that

$$\begin{aligned} \Delta T_a &= \Delta T_t - \Delta T_{tf} - \Delta T_r \\ \Delta q_a &= \Delta q_t - \Delta q_{tf} \end{aligned} \tag{2}$$

where ΔT and Δq are the changes in temprature and specific humidity, respectively, averaged over the MABL, and the subscripts a, tf, r and t refer to changes due to advection, turbulent fluxes, radiational cooling and the total change, respectively. Total change values were estimated from the 10:48 and 16:48 UTC *Moana Wave* soundings for an approximately constant

MABL depth of 500 m (Table 1). The increase in MABL temperature and moisture due to turbulent fluxes was estimated using the average observed surface fluxes for the 6-hr simulation period over a 500-m depth, assuming a typical MABL top entrainment/surface flux ratio of -0.2 for temperature, and zero for moisture (i.e., negligible MABL top moisture 'venting'). The effect of radiative cooling was set to a constant rate following Paltridge and Platt (1976) for average equatorial conditions. For model simulations, the effect of radiational cooling and temperature advection are combined.

4. Simulations and discussion

We focus on the role surface fluxes play in determining the ABL structure and on identifying deficiencies in the surface flux formulation and its transport throughout the ABL. The flux and profile observations allow us to determine if favorable atmospheric model response would remain favorable also in a couple ocean-atmosphere simulation (e.g. that the atmospheric response observed by Beljaars (1995) is also accompanied by accurate simulated surface fluxes). Comparisons with the zero-advection runs allows us to examine if, and to what degree the pure and interaction terms are sensitive to external (prescribed) forcings other than fluxes. In all figures that involve factor separation, H, L, T represent runs with sensible heat flux (H), latent heat flux (L) and momentum flux (T) acting alone (i.e., other fluxes turned off), respectively. Similarly, any combination of the above represents simulation with these factors jointly turned on, and the 0 case represents the base state (simulation with all fluxes turned off).

The potential temperature profile at six hours of model simulation time for both observed-flux-forced and modeled-flux-forced runs along with the observed profiles at initial and final times are shown in Figure 3 (upper eight panels) for the eight simulations needed to separate 3 factors. All profiles from simulations that include the sensible heat flux (H) show a difference of up to 0.5 C in the temperature profiles between model-flux-forced runs and observed-flux-forced runs, with the latter warmer and except for the lowest level, in better agreement with the observed profiles. This difference between model-flux-forced and observed-flux-forced runs is because the observed sensible heat flux is about twice the modelled sensible heat flux, though both fluxes are small (less than $10 W m^{-2}$). Yet this small difference

is enough to account for about $100m$ greater ABL growth at six hours for the observed-flux-forced case. The additional sensible heating at the surface for the observed-flux-forced case is primarily responsible for the warming of the entire ABL and without it there is very little evolution of the temperature profile which remains very close to the initial profile. The additional sensible heating is mixed throughout the entire ABL resulting in what appears to be an overestimation of the ABL depth (inspect the HLT panel in Figure 3). The lowest level temperature ($15m$) for both the observed-flux-forced and observed-flux-forced simulations is warmer than the observed ship deck temperature by up to one degree, depending on the simulation time (Figure 3, bottom panel). The results described here then point to probable deficiencies in the sensible heat flux parameterization and the modeled temperature response to it.

Inspection of the pure (H,L,T), dual interaction (HL, HT, LT) and triple interaction (HLT) terms for potential temperature from (1) (Figure 4) confirms that the main discrepancy between model-flux-forced and observed-flux-forced simulations is due to the sensible heat flux parameterization. The observed sensible heat fluxes directly (i.e., through the pure effect) warm low and middle ABL levels considerably more than the weaker model-calculated sensible heat flux. The differences between model-flux-forced and observation-flux-forced runs in the pure effect of latent heat (L) is small, and there is virtually no difference in momentum (T) fluxes between model-flux-forced and observed-flux-forced simulations. Differences in synergistic (higher order) effects between the two runs are limited to higher levels reflecting the growth and divergence of the small differences in boundary forcing away from the surface. For example, in the HL simulations the factor separation profile values for potential temperature are positive in the upper ABL and negative in the lower ABL (for both the model-flux-forced and observed-flux-forced runs). In this case the ABL mixing is stronger because both sensible and latent heat flux are turned on, but the mixing is over a deeper layer (the ABL is deeper) and the corresponding nonlocal mixing is weaker than for the H or L cases yielding the not-as-well-mixed potential temperature profiles (HL panel in Figure 3).

Figures 5 and 6 are the counterparts of Figures 3 and 4 for specific humidity profiles. Here the discrepancies between the observed-flux-forced and the

model-flux-forced simulations are primarily due to the interaction between the sensible and the latent heat flux forcings and, to a lesser degree, due to the pure effect of latent heat flux. While the difference in the sensible heat flux between the model-flux-forced and the observed-flux-forced cases at the surface is large (in a relative sense), it is small in an absolute sense (see Figure 1, lower panel) and its pure effect on humidity profile throughout the ABL is negligible. On the other hand, when combined with a modest difference in the latent heat flux between the two simulations, this difference in the sensible heat flux affects the humidity profile more. Evidence for the overprediction of ABL height and the growth of small differences away from the boundary is apparent in Figures 5 and 6 as well. The sharp gradient in specific humidity at the lowest level cannot be maintained by the model in either case (Figure 5). The model responds with vigorous mixing at the lowest level manifested as strong drying/moistening in the direct and indirect flux terms.

Figure 7 shows the ABL height for the different simulations along with the direct and synergistic net contribution of the surface fluxes to this integrated ABL feature. By inspecting the differences between the model-flux-forced and observed-flux-forced simulation results, it is apparent that the stronger observed sensible heat flux which dominated the differences in humidity and temperature profiles is also the cause of the deep (and perhaps overpredicted) ABL height in the observation forced simulation suggesting that the nonlocal mixing of heat and moisture may be too vigorous.

A direct comparison between the observed and simulated fluxes, temperature, and specific humidity near the surface (at 15 m, Figures 1, 3, 5) reveals that the model simulates a surface layer which is slightly warmer and dryer then observed, and underestimates sensible heat fluxes (although values are small for both model-flux-forced and observed-flux-forced cases). Model predicted latent heat fluxes, on the other hand agree well with the observations for most of the simulation period but tend to overestimate latent heat flux towards the end of the simulation. Forcing the observed sensible heat fluxes tends to warm and dry the surface layer more than observed.

The elaborate initialization procedure (i.e., previous section) provided us with numerous additional sensitivity tests. These additional sensitivity tests

indicate that, while the advective forcing profoundly affects the final simulated temperature and humidity profiles, it does not affect the pure and synergistic flux terms appreciably. This indicates that the temperature and humidity ABL profiles are not sensitive to synegism between advection and surface fluxes and the profound differences in the final profiles are mostly due to the direct (pure) advection effect. This is in contrast with the response of the integrated ABL height to the imposed advection. When the model is run without advective forcing, the relative importance of the pure and synergistic flux terms increases considerably. Thus, the imposed advection strongly influences the ABL depth both directly and indirectly through synergism with the flux forcing. In general, as the number of relevant factors being investigated increases, the role of any specific factor diminishes because the synergistic interactions with the new factors are extracted (Alpert *et al* 1995). Inspection of the temperature and humidity profiles (upper panels in Figures 3 and 5) reveals that the runs forced with the observed fluxes tend to slightly over-predict the MABL height. However, while no subsidence was specified in our cases, the uncertainty in an imposed subsidence rate is such that it could easily account for the entire difference.

5. Conclusions

The response of atmospheric boundary layer (ABL) properties to surface flux forcing in a column ABL model was tested. The TOGA-COARE measured fluxes and soundings were used to initiate and test the Oregon State University ABL model in the tropical convective regime. Recent experiments with general circulation model flux parameterization have shown great sensitivity of the simulated large scale circulation to the heat flux parameterization in these regimes but did not allow for detailed sensitivity studies of the ABL integrated properties response. We tested how the surface flux forcings influence the thermodynamic profiles of potential temperature and specific humidity throughout the MABL and determine its structure and depth. The method proposed by Stein and Alpert (1993) was used to investigate the manner by which the different forcings interact with each other to determine the ABL properties. Here we find that the main discrepancy between model-flux-forced and observed-flux-forced simulations is due to the sensible heat flux parameterization. The observed sensible heat fluxes directly (i.e.,

through the pure effect) warm low and middle ABL levels considerably more than the weaker model-calculated sensible heat flux. The differences between model-flux-forced and observation-flux-forced runs in the pure effect of latent heat (L) is small, and there is virtually no difference in momentum (T) fluxes between model-flux-forced and observed-flux-forced simulations. Differences in synergistic (higher order) effects between the two runs are limited to higher levels reflecting the growth and divergence of the small differences in boundary forcing away from the surface.

References

Alpert, P., M. Tsidulko, and U. Stein,1995: Can sensitivity studies yield absolute comparisons for the effects of several processes? *J. Atmos. Sci.*, bf 52, 597-601.

Beljaars, A. C. M., 1995: The parameterization of surface fluxes in large-scale models under free convection. *Quart. J. Roy. Meteorol. Soc.*, **121**, 255-270.

Businger, J. A., J. C. Wyngaard, Y. Izumi and E. F. Bradley, 1971: Flux-profile relationships in the atmospheric surface layer. *J. Atmos. Sci.*, **28**, 181-189.

Deardorff, J. W., 1966: The countergradient heat flux in the lower atmosphere and in the laboratory. *J. Atmos. Sci.*, **23**, 503-506.

Elliot W. P. and D. J. Gaffen, 1991: On the utility of radiosonde humidity archives for climate studies. *Bulletin Am. Meteor. Soc.*, **72**, 1507-1520.

Fairall, C., E. F. Bradley, J. S. Godfrey, G. A. Wick, J. B. Edson, and G. S. Young, 1996a: Cool skin and warm layer effects on sea surface temperature. *J. Geophys. Res.*, **101**, 1295-1308.

Fairall, C., E. F. Bradley, D. P. Rogers, J. B. Edson, and G. S. Young, 1996b: Bulk parameterization of air-sea fluxes for TOGA COARE. *J. Geophys. Res.*, **101**, 3747-3764.

Frech, M. and L. Mahrt, 1995: A two-scale mixing formulation for the atmospheric boundary layer. *Bound.-Layer Meteorol.*, **73**, 91-104.

Gordon, C., and R.A. Corry, 1991: A model simulation of the seasonal cycle

in the tropical Pacific Ocean using climatological and modeled surface forcing. *J. Geophys. Res.*, **96**, 847-864.

Hack, J. J., B. A. Boville, B. P. Briegleb, J. T. Kiehl, P. J. Rasch, and D. L. Williamson, 1993: Description of the NCAR community climate model (CCM2). NCAR technical note, NCAR/TN-382+STR, 108 pp.

Holtslag, A. A. M., 1987: Surface fluxes and boundary-layer scaling; models and applications. KNMI Sci. Rep. 87-02.

Holtslag, A. A. M. and B. Boville, 1993: Local versus nonlocal boundary-layer diffusion in a global climate model. *J. Climate*, **6**, 1825-1842.

Holtslag, A. A. M., E. I. F. de Bruijn and H.-L. Pan, 1990: A high-resolution air mass transformation model for short-range weather forecasting. *Mon. Wea. Rev.*, **118**, 1561-1575.

Holtslag, A.A.M. and M. Ek, 1996: The simulation of surface fluxes and boundary-layer development over the pine forest in HAPEX-MOBILHY. *J. Appl. Meteorol.*, **35**, 202-213.

Johnson, R. H., and P. Ciesielski, 1997: Documentation for CSU gridded analyses, and for IFA average fields. http://kiwi.atmos.colostate.edu/scm/toga-coare.html. Dept. Atmos. Sci., Colorado State University.

Latif, M., J. Biercamp and H. von Storch, 1988: Response of a Coupled Ocean-Atmosphere General Circulation Model to Wind Bursts. *J. Atmos. Sci.*, **45**, 964-979.

Miller, M.J., A.C.M. Beljaars and T.N. Palmer, 1992: The sensitivity of the ECMWF model to the parameterizations of evaporation from tropical oceans. *J. Climate*, **5**, 418-434.

Palmer T. N., and D.L.T. Anderson, 1995: The prospects for seasonal forecasting-a review paper. *Quart. J. Roy. Meteorol. Soc.*, **120**, 755-795.

Paltridge, G. W. and C. M. R. Platt, 1976: *Developments in Atmospheric Science, 5: Radiative processes in meteorology and climatology.* Elsevier Scientific Publ. Co., Amsterdam, 318 pp.

Paulson, C. A., 1970: The mathematical representation of wind speed and tmperature profiles in the unstable atmospheric surface layer. *J. Appl. Meteorol.*, 9, 857-861.

Smith, S. D., 1988: Coefficients for sea surface wind stress, heat flux and wind profiles as a function of wind speed and temperature. *J. Geophys. Res.*, 93, 15,467-15,472.

Stein, U. and P. Alpert, 1993: Factor separation in numerical simulations. *J. Atmos. Sci.*, 50, 2107-2115.

Troen, I. and L. Mahrt, 1986: A simple model of the atmospheric boundary layer: Sensitivity to surface evaporation. *Bound.-Layer Meteorol.*, 37, 129-148.

Figure legend

Figure 1. Time series of observed surface wind stress (upper panel), and latent (squares) and sensible (circles) heat fluxes (lower panel) for 10 January 1993 from *Moana Wave*. Model-calculated values (solid line) are shown for the six-hour simulation period (shaded region).

Figure 2. Upper 4 panels: wind profiles for the four radiosondes launches from the *Moana Wave* during 10 January 1993 showing the persistent low level jet. Lower two panels: time series for 10 January 1993 showing the $15 - m$ wind speed and direction observed by the *Moana Wave*. Shaded regions indicates model simulation period.

Figure 3. Upper 8 panels: observed potential temperature profiles for 10 January 1993 at 10:48 UT (open diamonds; simulation start time), and 16:48 UT (solid diamonds; simulation end time), and potential temperature from model simulations using model-calculated (solid line) and observed (dashed line) surface fluxes, for the different factor seperation tests (H=sensible heat flux on, latent heat flux off, surface stress off; L=latent heat flux on, sensible heat flux off, surface stress off; T=surface stress on, sensible heat flux off, latent heat flux off; etc). Lower panel: time series for 10 January 1993 showing the sea surface (squares) and 15-meter (circles) temperatures observed by the

Moana Wave, and modelled 15-meter temperature using model-calculated (solid line) and observed (dashed line) surface fluxes. Shaded region indicates model simulation period. See text for explanation.

Figure 4. Profiles of modelled potential temperature factor separation values using model-calculated (solid line) and observed (dashed line) surface fluxes, for the different factor seperation tests. See text for explanation.

Figure 5. Same as Figure 3, but for specific humidity.

Figure 6. Same as Figure 4, but for specific humidity.

Figure 7. (a) Atmospheric boundary-layer (ABL) height, and (b) ABL height factor separation values for the various factor separation tests. See text for explanation.

Appendix
OSU Atmospheric Boundary-Layer Model

The Oregon State University Atmospheric Boundary-Layer (OSU ABL) model is a one-dimensional (column) model that was developed to simulate turbulent mixing in both marine and terrestrial atmospheric boundary layers, suitable for inclusion in large-scale models. The ABL mixing scheme (Troen and Mahrt, 1986) includes both local (gradient) diffusion and nonlocal (boundary-layer scale) mixing; the nonlocal heat and moisture mixing has been updated following Holtslag and Boville (1993) for use in the NCAR CCM3 (Hack et al, 1993), and over the ocean is coupled with a parameterization of ocean surface fluxes.

Ocean surface fluxes

The ocean-surface flux scheme in the OSU model determines the surface heat fluxes and surface stress, and are expressed in a bulk-aerodynamic form as

$$H = \rho c_p C_h \mid U \mid (\theta_s - \theta) \quad (3)$$

$$LE = \rho L_v C_q \mid U \mid (q_s - q) \quad (4)$$

$$\tau = \rho C_m U^2 \quad (5)$$

where H and LE are the sensible and latent heat fluxes, respectively, and τ is the surface stress ($=\rho u_*^2$, where u_* is the surface friction velocity), ρ is air density, c_p is specific heat ($1004.5 Jkg^{-1}K^{-1}$) and L_v is latent heat ($2.5x10^6 Jkg^{-1}$), C_h, C_q, and C_m are the surface turbulent exchange coefficients for heat, moisture, and momentum, respectively (C_m is also called the *drag coefficient*, C_d), all functions of stability, defined below. (Here we adopt the usual convention that $C_q = C_h$.) $\theta_s - \theta$ and $q_s - q$ are the gradients in potential temperature and specific humidity, respectively, between the surface and a reference height in the atmosphere (e.g. the first atmospheric level in a model), U is the horizontal wind speed, and $\mid U \mid$ is the horizontal wind velocity scale which includes convection-induced large eddy motion defined as

$$\mid U \mid = u^2 + v^2 + (\beta w_*)^2 \quad (6)$$

where u and u are the horizontal wind components, β is an empirical coefficient set equal to 1.2 following Beljaars (1995), and w_* is the convective velocity scale.

The surface exchange coefficients for heat and momentum are

$$C_h = \frac{k^2}{[ln(z/z_{0m}) - \Psi_m(z/L)]\,[ln(z/z_{0h}) - \Psi_h(z/L)]} \quad (7)$$

$$C_m = \frac{k^2}{[ln(z/z_{0m}) - \Psi_m(z/L)]^2} \quad (8)$$

where k is the von Kármán constant (0.40), z is the atmospheric reference height, z_{0m} and z_{0h} are the roughness lengths for momentum and heat, respectively, L is the Obukhov length, and $\Psi_{m,h}$ are the stability profile functions for momentum and heat following Paulson (1970).

The roughness lengths for momentum and heat are defined as

$$z_{0m} = 0.11\nu/u_* + 0.018u_*^2/g \quad (9)$$

$$z_{0h} = 0.40\nu/u_* + 1.4x10^{-5} \quad (10)$$

following Smith (1988), where ν is the kinematic viscosity, and g is gravity.

Atmospheric boundary-layer mixing

The atmospheric boundary-layer scheme in the OSU model predicts tendencies of the potential temperature (θ), specific humidity (q), and horizontal components of the wind ($\vec{V}_h$) due to atmospheric turbulent mixing using a modified 'K' theory (Troen and Mahrt, 1986; Holtslag et al, 1990; Holtslag and Boville, 1993). The set of prognostic equations for heat, moisture, momentum, respectively, is

$$\frac{\partial\theta}{\partial t} = \frac{\partial}{\partial z}\left[K_h\left(\frac{\partial\theta}{\partial z} - \gamma_\theta\right)\right] + \vec{V}\cdot\nabla\theta + rad_T \quad (11)$$

$$\frac{\partial q}{\partial t} = \frac{\partial}{\partial z}\left[K_q\left(\frac{\partial q}{\partial z} - \gamma_q\right)\right] + \vec{V}\cdot\nabla q \quad (12)$$

$$\frac{\partial\vec{V}_h}{\partial t} = \frac{\partial}{\partial z}\left[K_m\left(\frac{\partial\vec{V}}{\partial z} - \gamma_m\right)\right] + \vec{V}\cdot\nabla\vec{V} \quad (13)$$

where K_h, K_q, and K_m are the eddy diffusivities for heat, moisture, and momentum, respectively, $\gamma_{\theta,q,m}$ are nonlocal (boundary-layer scale) mixing terms for heat, moisture, and momentum, respectively, and $\vec{V}$ is the three dimensional wind vector. Here we make the usual assumption of equating the diffusivity for moisture with that of heat, so that $K_q = K_h$. The advection terms, $\vec{V}\cdot\nabla\vec{V}, \theta, q$, and the radiative flux divergence term, rad_T, must be externally specified.

In the unstable case above the surface layer ($z > z_s \equiv 0.1h$), the eddy diffusivity for momentum is defined following Troen and Mahrt (1986)

$$K_m(z) = w_s k z \left(1 - \frac{z}{h}\right)^p \tag{14}$$

where w_s is the boundary layer velocity scale, k is the von Kármán constant (0.4), h is boundary-layer depth, and $p = 2$.

The boundary layer velocity scale is evaluated at the top of the surface layer and defined following a modification by Holtslag and Boville (1993)

$$w_s = u_* \phi_m^{-1} \left(\frac{z_s}{L}\right) \tag{15}$$

$$w_s = \left(u_*^3 + 15k\frac{z_s}{h}w_*^3\right)^{1/3} \tag{16}$$

where u_* is the surface friction velocity, ϕ_m is the nondimensional profile function for momentum (defined below), and L is the Obukhov length, defined as

$$L = -\theta_{av}\frac{u_*^3}{gk(\overline{w'\theta'_v})_s} \tag{17}$$

where θ_{av} is the virtual potential temperature at some atmospheric reference level, g is gravity, w_* is the convective velocity scale (defined below), and $(\overline{w'\theta'_v})_s$ is the surface virtual heat flux.

In the neutral limit, the velocity scale $w_s \rightarrow u_*$, while in the free convection case as wind speed vanishes, $w_s \rightarrow 0.84 w_*$, where the convective velocity scale is

$$w_* = \left[\frac{gh}{\theta_{av}}(\overline{w'\theta'_v})_s\right]^{1/3} \tag{18}$$

The eddy diffusivity for heat (K_h) is related to the eddy diffusivity for momentum in terms of the turbulent Prandtl number (Pr)

$$K_h = K_m Pr^{-1} \tag{19}$$

where the turbulent Prandtl number is

$$Pr = \frac{\phi_h(\frac{z_s}{L})}{\phi_m(\frac{z_s}{L})} + Ck\frac{w_*}{w_s}\frac{z_s}{h} \tag{20}$$

where C is a coefficient set to 7.2 following Holtslag and Boville (1993). Pr is determined as the value at the top of the surface layer ($z_s = 0.1h$) using surface-layer similarity theory and assumed constant above z_s. In the neutral limit, $Pr \rightarrow 1$; $Pr = 1.0$ for stable conditions. The nondimensional profile functions for temperature and momentum evaluated at z_s are defined as

$$\phi_h = \left\{ \begin{array}{ll} 6.0 & \text{very stable} \\ 1.0 + 5.0\frac{z}{L} & \text{stable} \\ \left(1.0 - 15\frac{z}{L}\right)^{-1/2} & \text{unstable} \end{array} \right\} \tag{21}$$

$$\phi_m = \left\{ \begin{array}{ll} 6.0 & \text{very stable} \\ 1.0 + 5.0\frac{z}{L} & \text{stable} \\ \left(1.0 - 15\frac{z}{L}\right)^{-1/3} & \text{unstable} \end{array} \right\} \tag{22}$$

These formulations are taken from Businger *et al* (1971) with modifications by Holtslag (1987). For the very stable case ($z/L > 1$), we set $z/L = 1$ so that the profile functions remain constant.

For the stable case, and in the surface layer in unstable conditions, $u_*\phi_m^{-1}(z/L)$ replaces w_s and the eddy diffusivity for momentum is

$$K_m = u_*\phi^{-1}\left(\frac{z}{L}\right) kz\left(1 - \frac{z}{h}\right)^p \tag{23}$$

where $\phi_{h,m}$ now depend on z/L instead of on z_s/L. As a modification to surface-layer similarity theory, the term $(1 - z/h)^p$ is included in the diffusivity for proper matching with the mixed layer ($z > z_s$).

The nonlocal terms ($\gamma_{\theta,q,m}$) represent mixing on the boundary-layer depth scale. γ_θ is sometimes called 'counter-gradient' because nonlocal mixing in the upper convective boundary layer can often be up-gradient (Deardorff, 1966). $\gamma_{\theta,q}$ are zero in stable and neutral conditions, and in unstable conditions $[(\overline{w'\theta'_v})_s > 0]$ defined as

$$\gamma_\theta = C w_* \frac{(\overline{w'\theta'})_s}{w_s^2 h} \tag{24}$$

$$\gamma_q = C w_* \frac{(\overline{w'q'})_s}{w_s^2 h} \tag{25}$$

where $(\overline{w'\theta'})_s$ and $(\overline{w'q'})_s$ are the surface heat and moisture flux (in kinematic units), respectively. A similar expression for the nonlocal mixing of momentum has been explored by Frech and Mahrt (1995), but is not included because its generality has not been rigourously examined, so γ_m is set to zero.

The boundary-layer height is diagnosed as

$$h = \frac{Ri_{cr}|\vec{V}(h)|^2}{(g/\theta_{av})(\theta_v(h) - \theta^*_{av})} \tag{26}$$

where Ri_{cr} is the critical Richardson number, θ_{av} is the reference virtual potential temperature at the first model above the surface, g is the gravity, $\theta_v(h)$ is the virtual potential temperature at model level h, and $|V(h)|$ is the magnitude of the horizontal wind at level h. This approach to diagnosing the boundary-layer height (following Troen and Mahrt, 1986; Holtslag and Boville, 1993) also requires the specification of a low-level potential temperature (θ^*_{av}) which is defined as

$$\theta^*_{av} = \left\{ \begin{array}{ll} \theta_{av} & \text{stable} \\ \theta_{av} + C\frac{(\overline{w'\theta'_v})_s}{w_s} & \text{unstable} \end{array} \right\} \tag{27}$$

When the boundary layer is unstable, the virtual potential temperature above the surface in (27) is enhanced by thermal effects in an amount that is proportional to the surface sensible heat flux. In the neutral limit as $\overline{w'\theta'_v})_s \rightarrow 0$, $w_s \rightarrow u_*$, and $\theta^*_{av} \rightarrow \theta_{av}$.

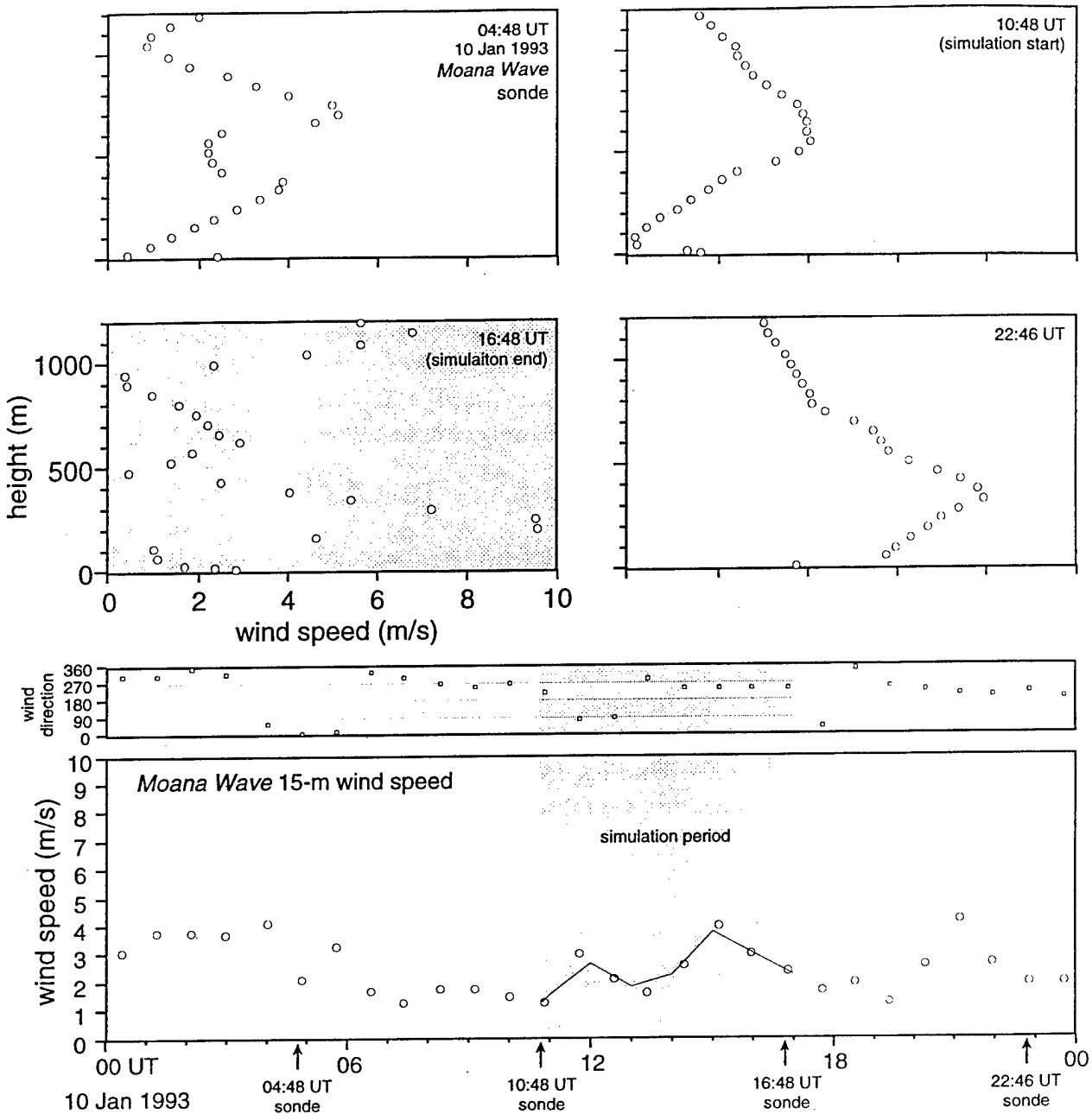
04:48 UT
10 Jan 1993
Moana Wave
sonde
10:48 UT
(simulation start)
16:48 UT
(simulaiton end)
22:46 UT
height (m)
1000
500
0
0
2
4
6
8
10
wind speed (m/s)
wind direction
360
270
180
90
0
Moana Wave 15-m wind speed
simulation period
wind speed (m/s)
10
9
8
7
6
5
4
3
2
1
0
00 UT
10 Jan 1993
06
12
18
00
04:48 UT sonde
10:48 UT sonde
16:48 UT sonde
22:46 UT sonde

Figure 1

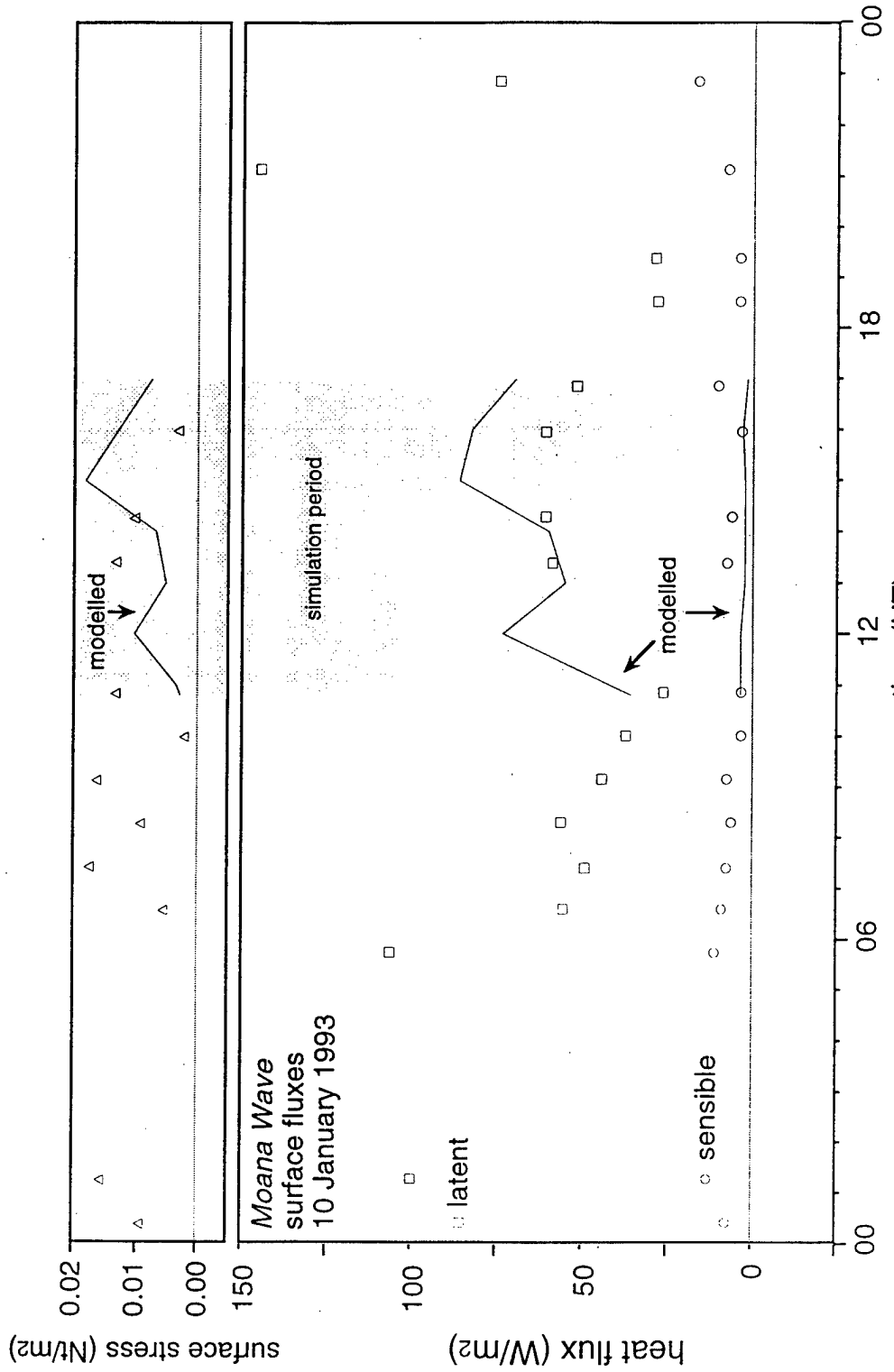
surface stress (Nt/m2)
0.02
0.01
0.00
modelled
heat flux (W/m2)
150
100
50
0
Moana Wave
surface fluxes
10 January 1993
simulation period
latent
sensible
modelled
00
06
12
18
00
time (UT)

Figure 2

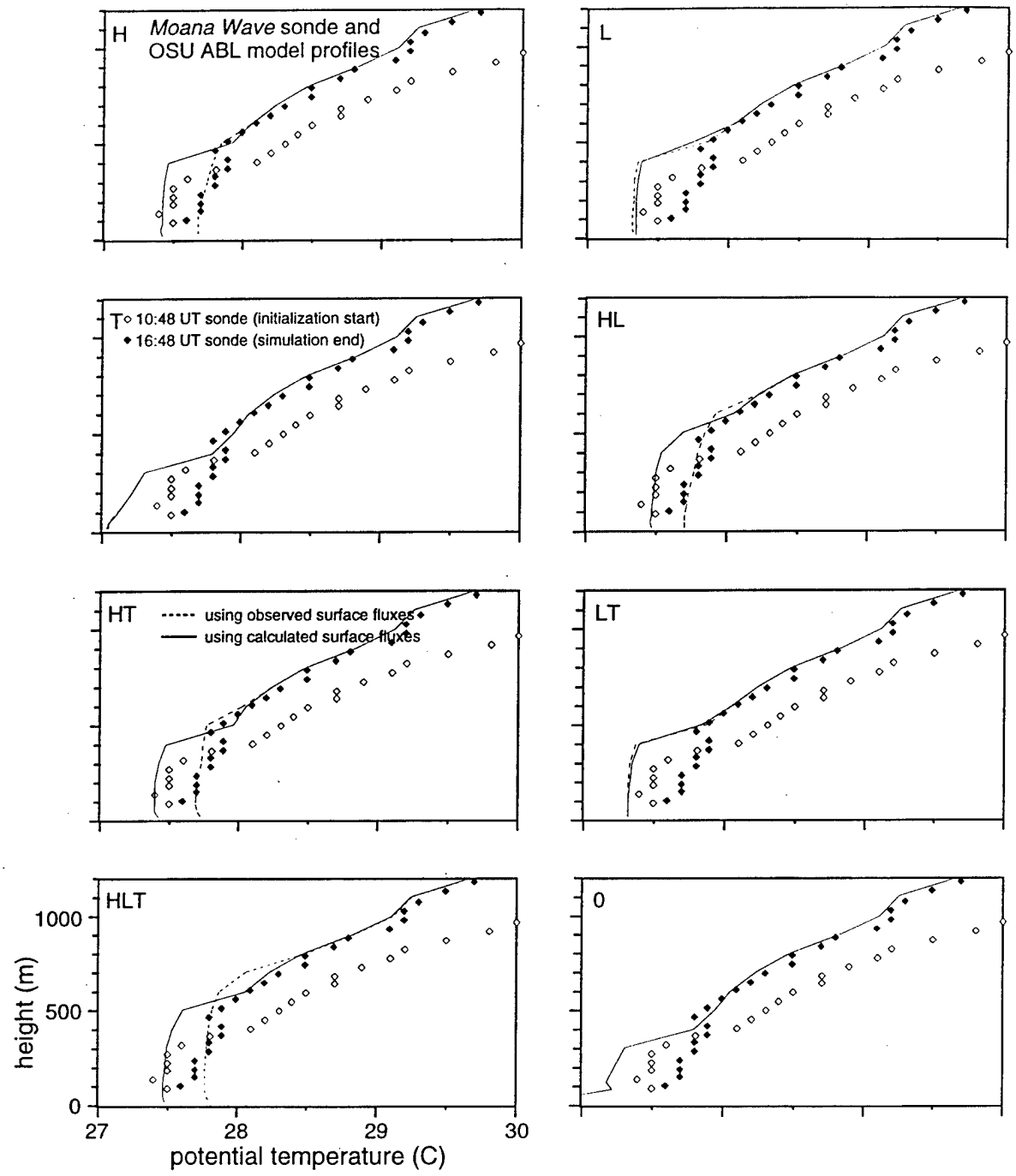

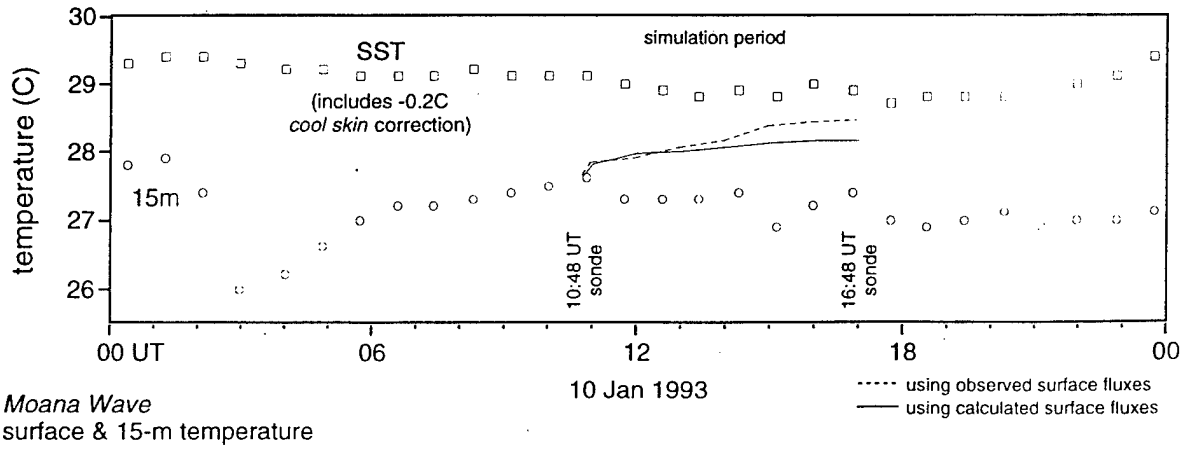

Moana Wave
surface & 15-m temperature

Figure 3

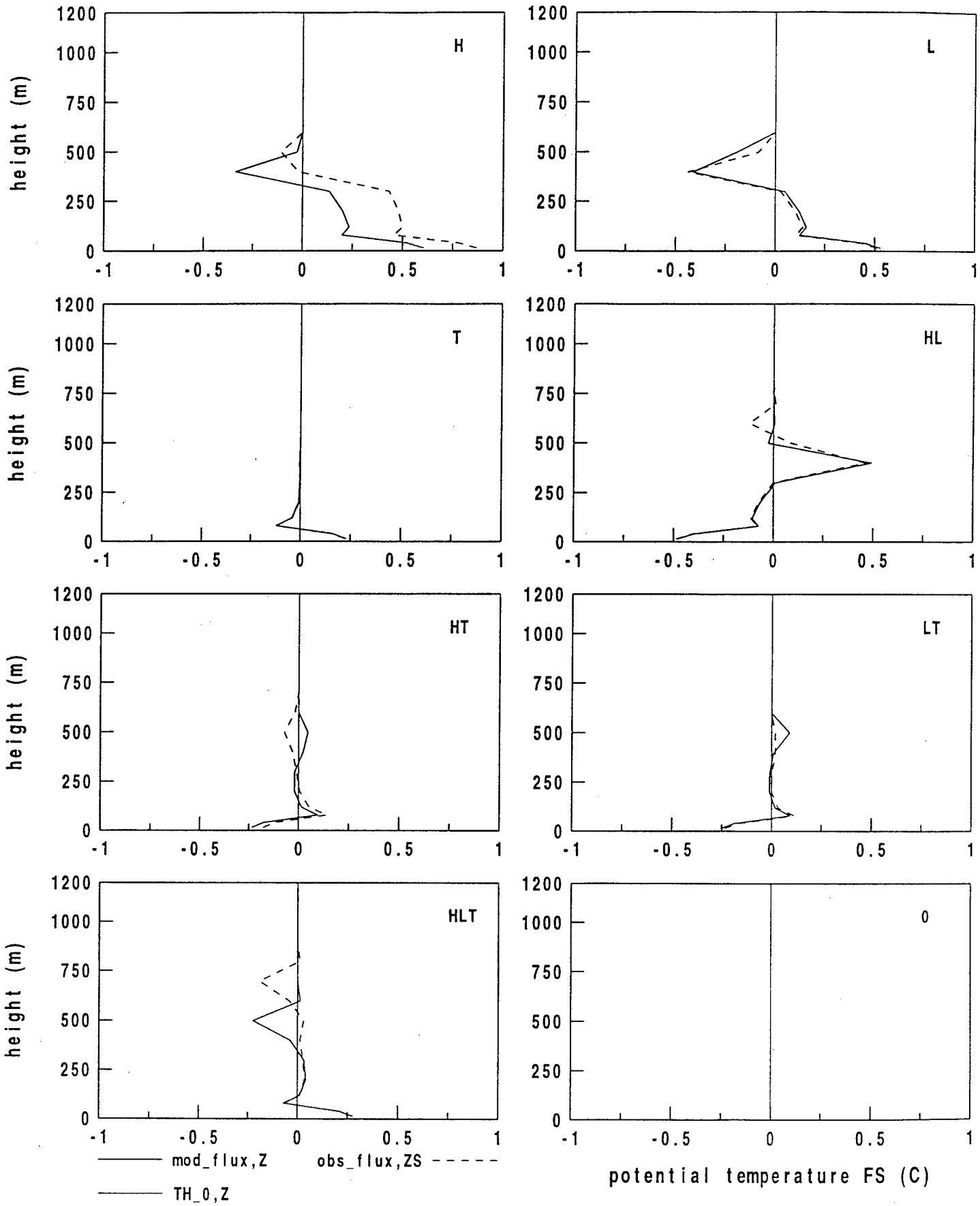
TOGA-COARE, Moana Wave, 10 Jan 93, OSU ABL 6-hr model simulation
height (m)
1200
1000
750
500
250
0
-1
-0.5
0
0.5
1
H
L
T
HL
HT
LT
HLT
0
mod_flux,Z
obs_flux,ZS
TH_0,Z
potential temperature FS (C)

Figure 4

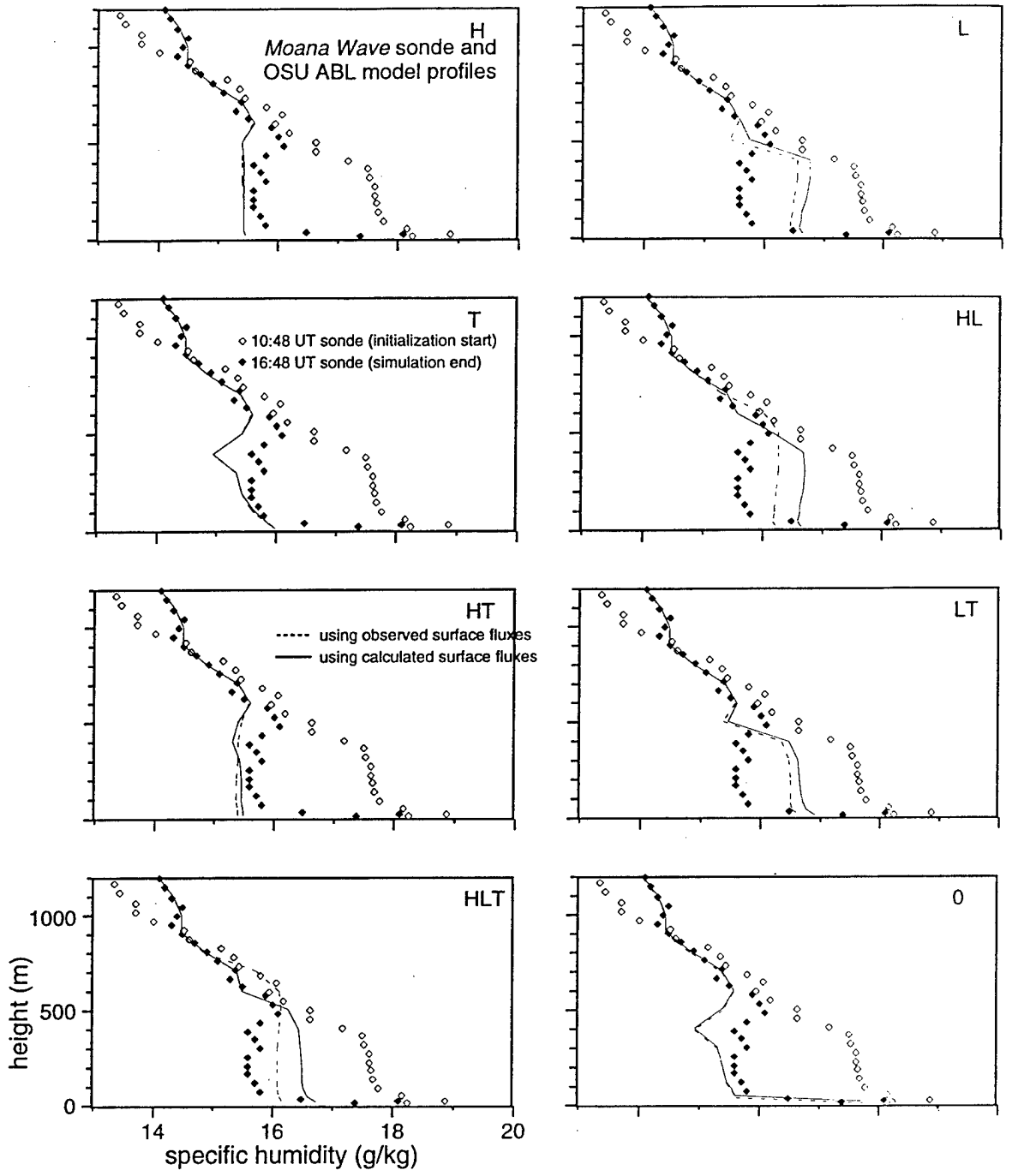

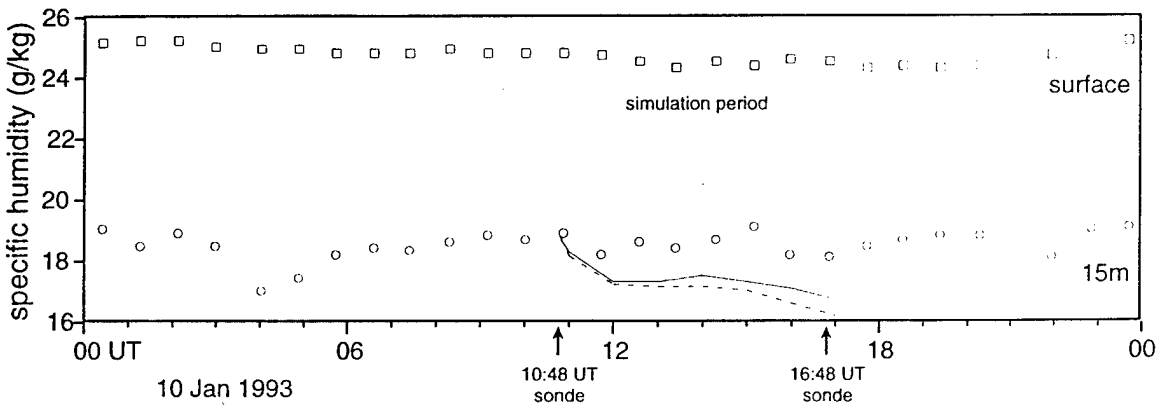

Moana Wave
surface & 15-m specific humidity

Figure 5

Moana Wave, 10 Jan 93, OSU ABL 6-hr model simulation

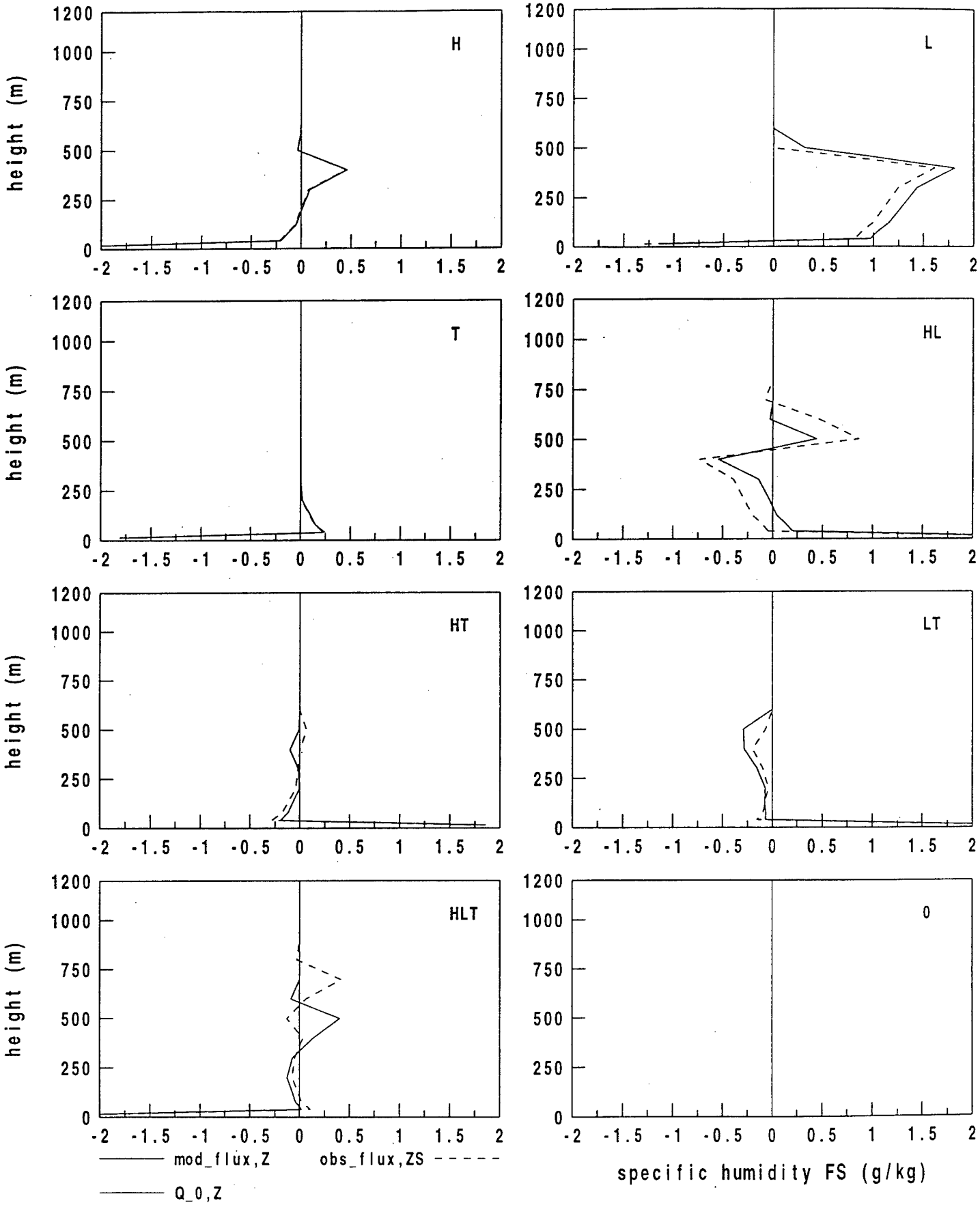

Figure 6

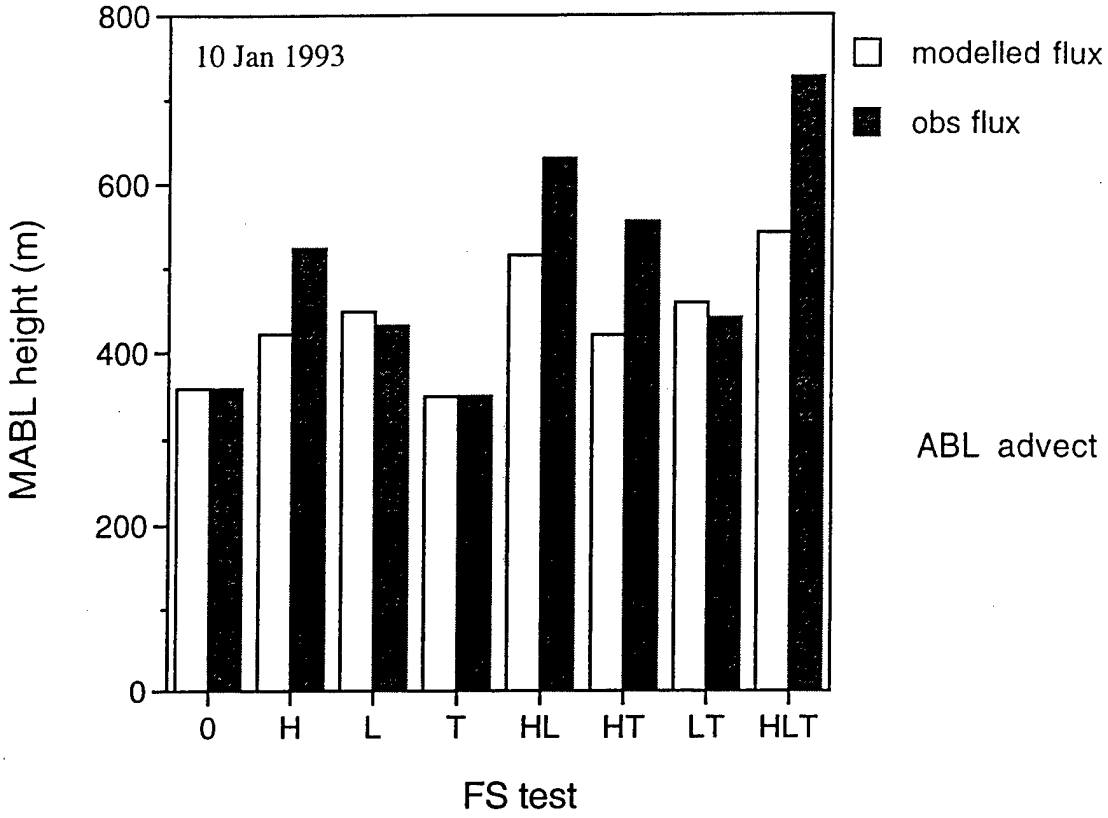
10 Jan 1993
MABL height (m)
800
600
400
200
0
0
H
L
T
HL
HT
LT
HLT
FS test
modelled flux
obs flux
ABL advect

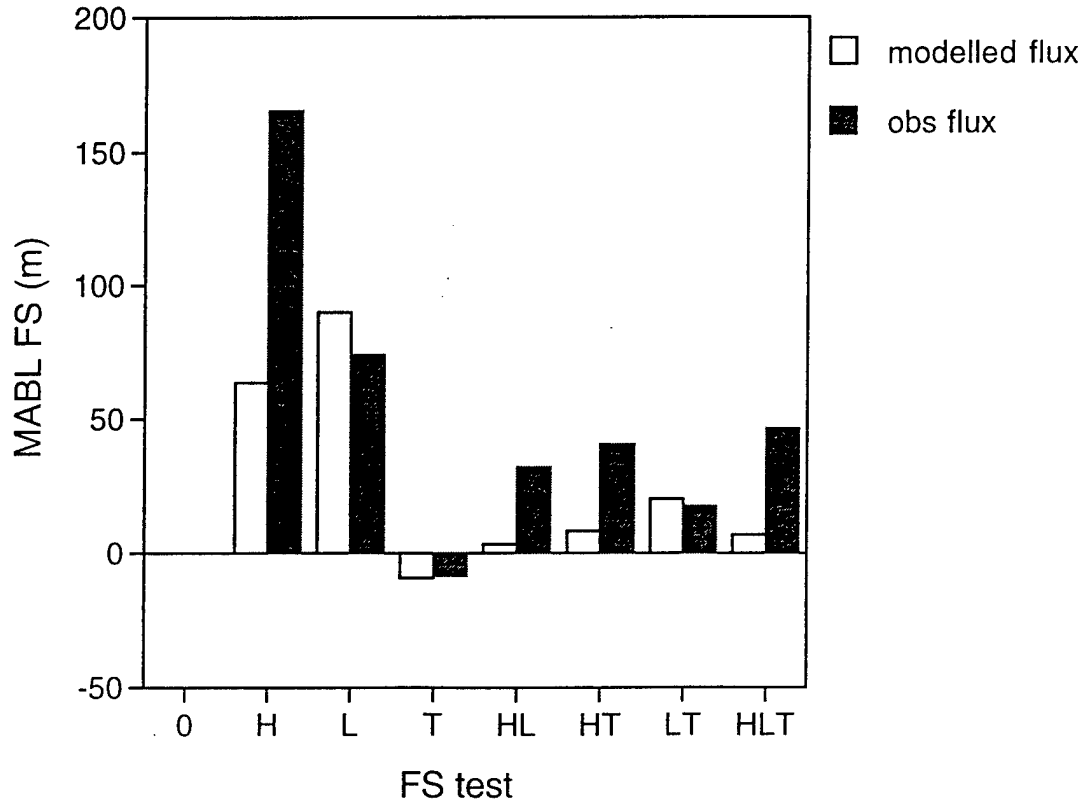
MABL FS (m)
200
150
100
50
0
-50
0
H
L
T
HL
HT
LT
HLT
FS test
modelled flux
obs flux

Figure 7

5.
A top-hat formulation for boundary-layer cloud cover

1. Introduction

We update the formulation for boundary-layer clouds described in Ek and Mahrt (1991; hereafter EM91) using a formulation based on specific humidity rather than relative humidity. Subgrid variability of boundary-layer moisture complicates the formulation of boundary-layer cloud cover. When spatial fluctuations of moisture are large, boundary-layer clouds first form at a lower spatially averaged humidity. The analysis of EM91 indicates that subgrid variations of moisture exert a much greater influence on cloud development than subgrid variations of temperature. Although this analysis is based upon only one field program, we take advantage of this potential simplification and neglect subgrid variations of temperature. To examine the feasibility of the specific humidity approach, we evaluate the cloud cover formulation which uses horizontal variability of specific humidity, and compare it with the corresponding cloud cover formulation by EM91 which uses the horizontal variability of relative humidity.

2. Fractional cloud cover

We formulate subgrid variations of moisture (specific humidity) in the simplest possible manner by dividing the grid area into two subregions, a drier cloud-free subgrid region (q_d) and a moister cloudy subgrid region (q_m). The grid-averaged moisture is

$$q = (1 - A_c)q_d + A_c q_m \tag{1}$$

where A_c is the fractional cloud cover for the grid box. We assume a top hat distribution of moisture (Le Treut, 1985) which in practice performs nearly as well as the more realistic Gaussian distribution (EM91) or a triangular distribution (Smith, 1990), and is more computationally efficient. For example, a top hat distribution and total variation $2\Delta q$ (Figure 1), the cloud cover is simply

$$A_c = \frac{0.5(q + \Delta q - q_s)}{\Delta q} \tag{2}$$

where q_s is the saturation specific humidity, a function of temperature only.

Given a model prediction for q, q_s, and Δq, and referring to Figure 1, the total water specific humidity in the cloudy subgrid region ranges from q_s to $q + \Delta q$ with an average value of

$$q_m = 0.5(q + \Delta q + q_s) \tag{3}$$

Similarly, the average total water specific humidity of the clear subgrid region is

$$q_d = 0.5(q - \Delta q + q_s) \tag{4}$$

The average liquid water (in the cloudy subgrid region only) is then

$$q_l = q_m - q_s \tag{5}$$

Note that cloud cover may be defined in terms of average liquid water by combining (2) and (5) so

$$A_c = \frac{q_l}{\Delta q} \tag{6}$$

Also note that in the limit of no cloud cover, $A_c = 0$ when $q + \Delta q \leq q_s$, then

$$\begin{aligned} q_l &\rightarrow 0 \\ q_d &\rightarrow q \\ q_s, q_m &\rightarrow q + \Delta q \end{aligned} \tag{7}$$

Similarly, for complete overcast, $A_c = 1$ when $q - \Delta q \geq q_s$, then

$$\begin{aligned} q_l &\rightarrow \Delta q \\ q_d, q_s &\rightarrow q - \Delta q \\ q_m &\rightarrow q \end{aligned} \tag{8}$$

The lowest implied cloud base within the grid area occurs where q_s first decreases to $q + \Delta q$, that is, where q_l is first nonzero. The implied cloud cover increases with height up to the model level just below the boundary-layer top, but for simplicity we assume that the cloud cover fraction is equal to the maximum value in the cloud layer and is constant with height between the cloud base and boundary-layer top. This maximum cloud cover can then be used in determining the radiation budget at the surface (or with a more sophisticated radiation scheme), and with a enhanced cloud mixing formulation (if present). Obviously more complex formulations would be more realistic but are not adopted here for simplicity.

We make use of the HAPEX-MOBILHY aircraft data set used in EM91 to evaluate the new cloud cover formulation given the observed specific humidity variation. Assuming an adiabatic temperature decrease with height from the aircraft level to the cloud base above, we determine the saturation specific humidity (q_s) decrease, while the actual specific humidity (q) is assumed to remain constant. The cloud cover predicted by (2) based on a top-hat distribution of specific humidity is shown in Figure 2, and compares similarly with the formulation based on gaussian distribution of relative humidity (also shown; i.e. from Figure 6 in EM91).

3. Subgrid variation of moisture

The subgrid variability of total water specific humidity (Δq) involves both turbulent scale variations and those mesoscale variations not resolved by the horizontal grid of large-scale models. For simplicity, we assume that the turbulent and mesoscale variations are uncorrelated so that the magnitude of Δq is the square root of the sum of the turbulent variation of total water specific humidity and a more empirical expression for the mesoscale variation.

$$\Delta q = (\Delta q_{turb}^2 + \Delta q_{meso}^2)^{0.5} \tag{9}$$

turbulent scale variation

The specific humidity variation (turbulent scale) at the boundary-layer top is defined as

$$\Delta q_{turb} = \sqrt{3}\sigma_{q_{turb}} \tag{10}$$

where $\sigma_{q_{turb}}$ is the standard deviation of specific humidity (turbulent scale), and the factor $\sqrt{3}$ relates $\sigma_{q_{turb}}$ to Δq_{turb} for a top-hat moisture distribuiton. Further, $\sigma_{q_{turb}}$ is defined as

$$\sigma_{q_{turb}} = \frac{(\overline{w'q'})}{\sigma_w r_{wq}} \tag{11}$$

where $\overline{w'q'}$ is the moisture flux, σ_w is the vertical velocity variance, r_{wq} is the correlation between vertical velocity and specific humidity, and all terms are evaluated at the boundary-layer top. In simple boundary-layer models, $\overline{w'q'}$ and σ_w are normally available, while r_{wq} is not. A simplified expression for the specific humidity variation is then

$$\Delta q_{turb} = \frac{C(\overline{w'q'})}{\sigma_w} \tag{12}$$

where C is a coefficient that absorbs the $\sqrt{3}$ factor in (10) and assumes a constant value for r_{wq} (=0.3 as suggested by analysis of the HAPEX-MOBILHY data, so that $C = 5.77$). Comparison of the observed specific humidity variation (Δq) with that predicted by (12) shows a good correlation (Figure 3).

mesoscale variation

The expression for the mesoscale moisture variability is given as

$$\Delta q_{meso} = a_0 - a_1 \log(\Delta x) \tag{13}$$

where $a_0 = -0.254$, $a_1 = 0.445 km^{-1}$, and Δx is the horizontal grid scale (in kilometers), and has been derived from the empirical expression for the mesoscale relative humidity variance ($\sigma^2_{RH_{meso}}$) in EM91, and is shown in Figure 4 (similar to Figure 9 in EM91).

4. Summary

The cloud cover formulation by Ek and Mahrt (1991) based on a gaussian distribution of relative humidity is modified to take advantage of a simpler top-hat distribution of specific humidity. Results using an aircraft data set from the HAPEX-MOBILHY field program indicate that the specific-humidity top-hat distribution approach is a suitable alternative to the relative humidity gaussian distribution approach, and should be examined further with data

sets from other field programs, and tested coupled in a boundary-layer model (e.g. the OSU atmospheric boundary-layer model; Troen and Mahrt, 1986).

References

Ek, M. and L. Mahrt, 1991: A formulation for boundary-layer cloud cover. *Ann. Geophysicae*, 9, 716-724.

Le Treut, H., 1985: Cloud prediction experiments with the LMD GCM. In 'Workshop on cloud cover parameterization in numerical models', pp. 65-86. 26-28 November 1984. ECMWF Reading, England.

Smith, R.N.B., 1990: A scheme for predicting layer clouds and their water content in a general circulation model. *Q. J. R. Meteor. Soc.*, **116**, 435-460.

Troen, I. and L. Mahrt, 1986: A simple model of the atmospheric boundary layer: Sensitivity to surface evaporation. *Bound.-Layer Meteorol.*, **37**, 129-148.

Figure legend

Figure 1. Schematic of cloud cover formulation with grid-average total water specific humidity (q) and subgrid variation of specific humidity (Δq), with clear and cloudy subgrid regions for fractional boundary-layer cloud cover (a) less than 0.5, and (b) greater than 0.5.

Figure 2. Cloud cover calculated from (2) using observed values of height-adjusted specific humidity (q) and Δq versus observed cloud cover determined from aircraft radiation data for 18 upper-level flight legs from ten days in HAPEX-MOBILHY.

Figure 3. Relationship between the turbulent variance of specific humidity and the term on right hand side in (12).

Figure 4. Logarithmic least squares fit of the mesoscale standard deviation of specific humidity to the horizontal averaging length.

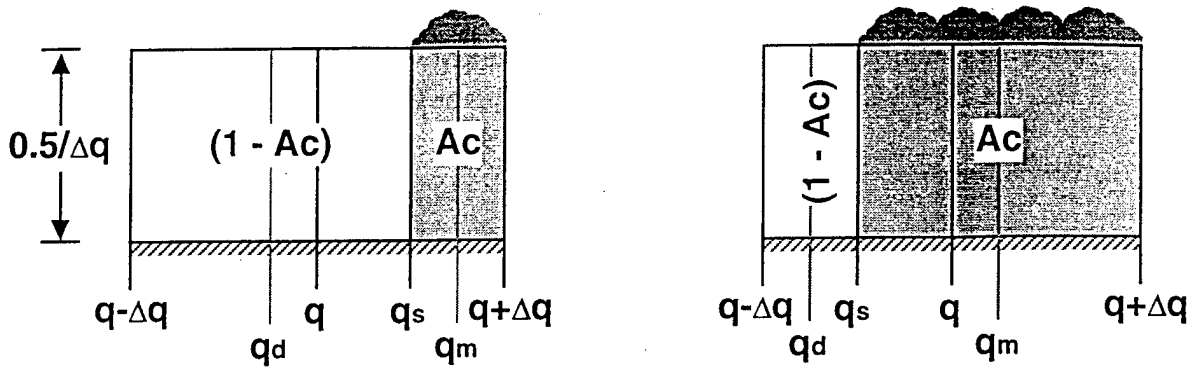

Figure 1

■ RH-based gaussian dist'n

□ specific-humidity-based top-hat dist'n

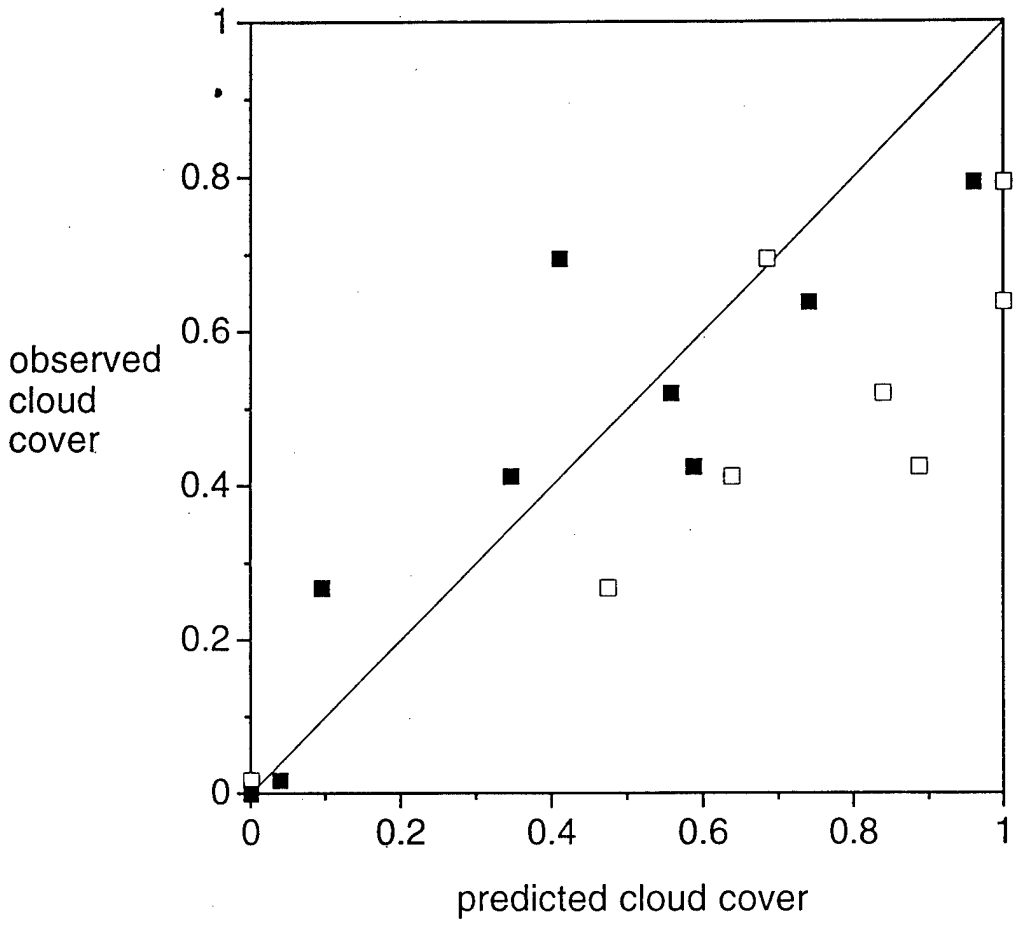

Figure 2

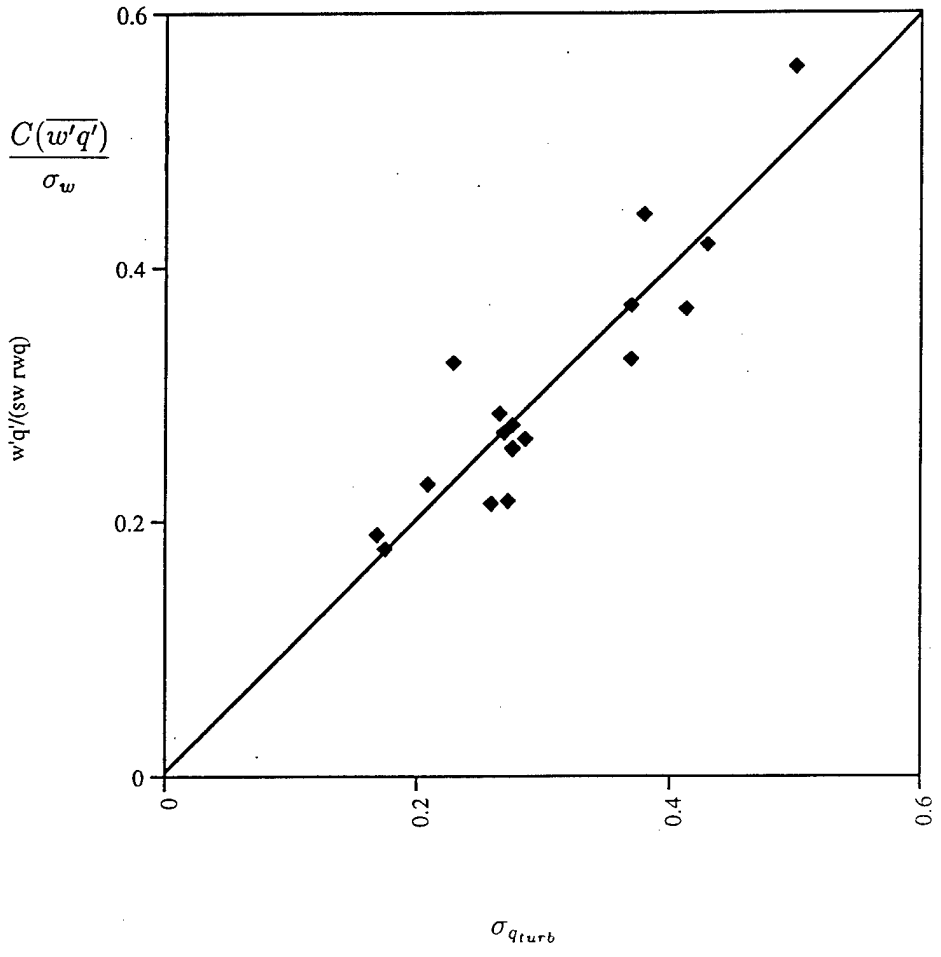
0.6
0.4
0.2
0
0
0.2
0.4
0.6
$\frac{C(\overline{w'q'})}{\sigma_w}$
w'q'/(sw rwq)
$\sigma_{q_{turb}}$

Figure 3

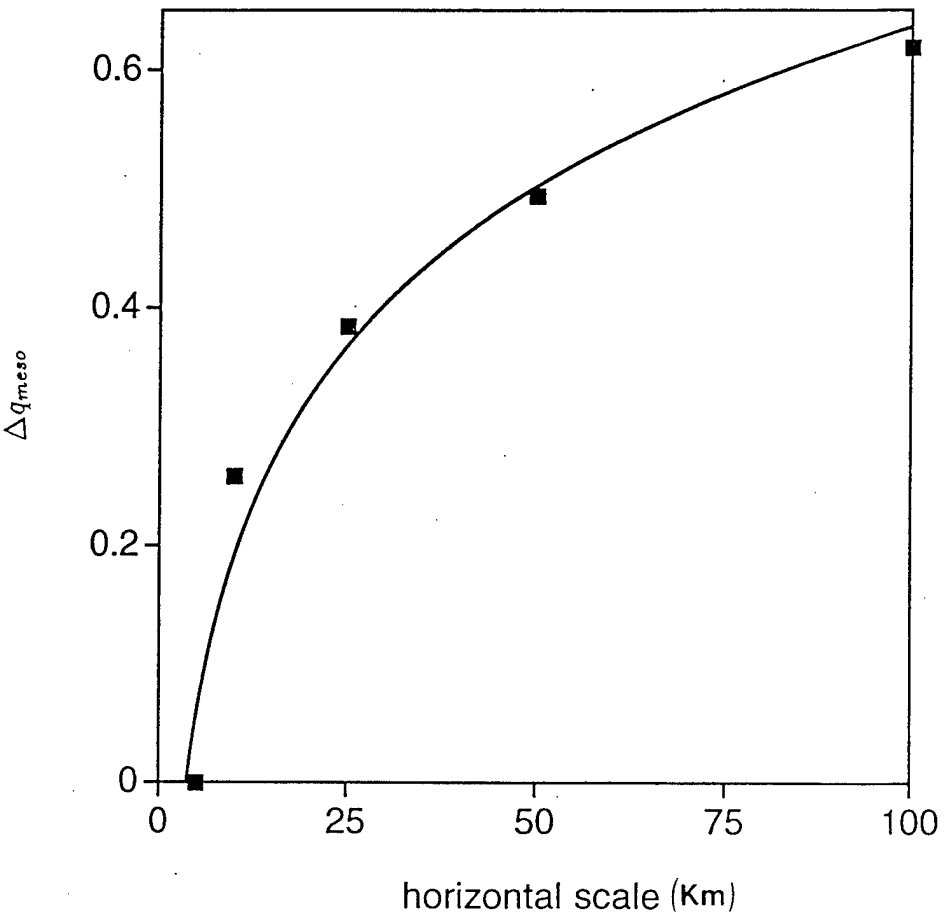

Figure 4

6.
The OSU atmospheric boundary-layer model land-surface scheme in PILPS testing

The land-surface scheme in the Oregon State University (OSU)Atmospheric boundary layer - Plant - Soil (CAPS) model has been tested as part of the Project for Intercomparison of Land-surface parameterization schemes (PILPS; Henderson-Sellers et al. 1993, 1995; Pitman et al. 1993). PILPS is a cooperative effort within the worldwide atmospheric/land-surface modeling community, and has been designed to test and compare many different land-surface parameterization schemes using different annual numerical and observational data sets. The goal is to examine and validate land-surface parameterizations used to simulate land-surface processes (surface evaporation, heat fluxes, soil temperature and moisture, etc) relevant for use in (coupling with) large-scale numerical weather prediction and global climate models.

In cooperation with Dr. Sam Chang at Phillips Laboratory (Hanscom AFB, Mass.), and others using some form of the OSU ABL land-surface scheme (i.e. the Eta model at the National Weather Service - National Centers for Environmental Prediction - Environmental Modeling Center, and the CAPS model at Lawrence Livermore National Laboratory), we have been making enhancements to the OSU CAPS model land-surface scheme through our participation in PILPS.

PILPS phase 2(a)

As part of PILPS phase 2(a) (Chen et al. 1997; Qu et al. 1998), land-surface simulations were made for the Cabauw tower site in central Netherlands. The Cabauw region is agricultural with many grass fields and scattered canals, and has rather simple hydrology since the soil is rarely moisture-stressed due to ample year-round precipitation and regulation of canal water. Nevertheless, there was still a wide variation in model results (surface fluxes, soil moisture content, etc) between the 24 participating schemes.

Specific to the OSU CAPS model, our canopy conductance (plant regulation of moisture flux) was initially constant except for a dependence of soil moisture content, and generally resulted in an overprediction in evaporation, and a corresponding underprediction in the sensible heat flux and surface temperature, affecting diurnal to annual results. The use of sub-diurnal (hourly or less) time steps, and the variability and nonlinear nature of the canopy conductance on a diurnal (and annual) basis precludes the use of a lower fixed canopy conductance to ameliorate the problem. Therefore, following the latest philosophy appropriate for use in the OSU CAPS land-surface scheme, a canopy conductance formulation that responds to atmospheric and soil (moisture) forcing was adopted (i.e. Noilhan and Planton, 1989) and is still under refinement.

Tests using this new canopy conductance formulation gives more realistic results. The computational expense of this canopy conductance formulation is minimal and has been adopted in the land-surface scheme.

An additional problem presented itself under snow-cover conditions, where temperatures were unrealistically low and the snowpack too persistent; this was resolved through a re-examination of the specified longwave albedo.

A study by Chang et al. (1998) was recently completed which examines the annual evolution of surface fluxes and other land-surface processes in response to atmospheric forcing as part PILPS phase 2(a) using the Cabauw data set. This manuscript gives a detailed description of model physics currently in the OSU CAPS land-surface scheme and a more comprehensive account of model simulations using the Cabauw data set. Such a manuscript is timely as it has been about ten years since a manuscript describing the land-surface scheme appeared (Pan and Mahrt, 1987), and many changes have been made since then.

Four manuscripts resulted from PILPS phase 2(a) work:

Chang, S. and M. Ek, 1996: Sensitivity study of the CAPS model land-surface scheme using the 1987 Cabauw/PILPS data set. *Phys. Chem. Earth*, **21**, 205-210.

Chang, S., D. Hahn, C.-H. Yang, D. Norquist, and M. Ek, 1998: Validation study of the CAPS model land-surface scheme using the 1987 Cabauw/PILPS data set. *J. Appl. Meteorol.* (to appear).

Chen, T., Henderson-Sellers, A., Milly, P., Pitman, A., Beljaars, Chang, S., Ek, M., and collaborators, 1997: Cabauw Experimental Results from the Project for Intercomparison of Landsurface Parameterization Schemes (PILPS). *J. Climate*, **10**, 1194-1215.

Qu, W., Henderson-Sellers, A., Pitman, A., Chang, S., Ek, M., and collaborators, 1998: Sensitivity of latent heat flux from PILPS land-surface schemes to perturbations of surface air temperature, *J. Atmos. Sci.*, **55**, 1909-1927.

PILPS phase 2(c)

At part of PILPS phase 2(c), 16 schemes participated, with land-surface simulations extended to a large horizontal domain of the Red-Arkansas River Basins, approximately 10^6 square km, consisting of about 100 grid points, with integrations extended to a 10-year period (using 1-hr time steps) in order to examine the hydrological perspective of long-term/large-spatial scale land-surface modeling. (These calculations required the use of a super computing facility, i.e. at CEWES, Vicksburg, MS.) During this phase of PILPS, we found that increasing the number of soil layers in the land-surface scheme from two to four with a shallow top layer (i.e. 3-cm), and including a root density function and a subroot zone, leads to better estimates of moisture and heat transport at the surface (both to/from the atmosphere and within the soil).

Including a shallow upper soil layer captures the sharp temperature and moisture gradients which exist in the soil near the surface, and can be particularly important where there is a substantial fraction of the surface covered by bare soil. For bare soil, the transfer of moisture to the atmosphere (bare soil evaporation) is a function of the hydraulic conductivity and the moisture gradient between the soil and the surface. Since the hydraulic conductivity is a highly nonlinear function of soil moisture content, as the soil dries out near the surface, the hydraulic conductivity is dramatically reduced and the bare soil evaporation diminishes rapidly. So if an upper soil layer is specified as too deep, the bare soil evaporation will generally be overestimated. (During precipitation events, the bare soil evaporation will be initially underestimated since the soil moisture content near the soil surface will be less with a deeper upper soil layer.) A subroot zone is also included, which provides a reservoir of moisture that is available for recharge of the root zone, that is, an upward movement of soil moisture from the subroot zone will occur as the root zone dries out. The trade-off in including more soil layers is a better representation of gradients and thus movement of heat and moisture in the soil versus an increase in computational time.

Specifying fractional root density which is not simply weighted by the fractional soil depth increases the importance of a particular layer in the calculation of transpiration (i.e. in an older version of the OSU CAPS model land-surface scheme). A nonuniform fractional root density leads to non-uniform soil moisture depletion in the root zone, which is realistic in that plant roots are often concentrated near the surface.

Three manuscripts resulted from PILPS phase 2(c) work:

Wood, E. F., D. P. Lettenmaier, X. Liang, D. Lohmann, S. Chang. M. Ek, and collaborators, 1998: The Project for Intercomparison of Land-surface Parameterization Schemes (PILPS) Phase 2(c) Red-Arkansas River Basin Experiment: 1. Experiment Description and summary intercomparisons. *J. Global and Planetary Change* (to appear).

Liang, X., E. F. Wood, D. P. Lettenmaier, D. Lohmann, S. Chang, M. Ek, and collaborators, 1998: The Project for Intercomparison of Land-surface Parameterization Schemes (PILPS) Phase 2(c) Red-Arkansas River Basin Experiment: 2. Spatial and temporal analysis of energy fluxes. *J. Global and Planetary Change* (to appear).

Lohmann, D., D. P. Lettenmaier, X. Liang, E. F. Wood, S. Chang, M. Ek, and collaborators, 1998: The Project for Intercomparison of Land-surface Parameterization Schemes (PILPS) Phase 2(c) Red-Arkansas River Basin Experiment: 3. Spatial and temporal analysis of water fluxes. *J. Global and Planetary Change* (to appear).

Other PILPS phases

Do to personnel and time limitations, we did not participate in PILPS phases 2(b), soil moisture simulation using HAPEX-MOBILHY data (Shao et al. 1994), or PILPS phase 2(d), land-surface simulations in a snow-dominated environment in boreal Russia (Schlosser et al. 1998).

Other references

Henderson-Sellers, A., A. J. Pitman, P. K. Love, P. Irannejad, and T. H. Chen, 1995: The Project for Intercomparison of Land-surface Parameterization Schemes (PILPS): Phases 2 & 3. *Bull. Amer. Meteor. Soc.*, **76**, 489-503..

Henderson-Sellers, A., Z.-L. Yang, and R. E. Dickinson, 1993: The Project for Intercomparison of Land-surface Parameterization Schemes (PILPS). *Bull. Amer. Meteor. Soc.*, **74**, 1335-1349.

Noilhan, J. and S. Planton, 1989: A simple parameterization of land surface processes for meteorological models. *Mon. Wea. Rev.*, **117**, 536-549.

Pan, H.-L. and L. Mahrt, 1987: Interaction between soil hydrology andboundary-layer development. *Boundary-Layer Meteorol.*, **38**, 185-202.

Pitman, A. J., A. Henderson-Sellers, M. Ek, M. Frech, L. Mahrt and collaborators, 1993: Project for Intercomparison of Land-surface Parameterizations Schemes (PILPS): Results from off-line control simulations (phase 1a). World Climate Research Programme (WCRP), Global Energy and Water Cycle Experiment (GEWEX), International GEWEX Project Office (IGPO), Publication Series No. 7, Dec. 1993.

Schlosser, C. A., Slater, A. G., Robock, A., Pitman, A. J., Vinnikov, K. Y., Henderson-Sellers, A., Speranskaya, N. A., Mitchell, K., Boone, A., Braden, H., Cox, P., DeRosney, P., Desborough, C. E., Dai, Y.-J., Duan, Q., Entin, J., Etchevers, P., Gedney, N., Gusev, Y. M., Habets, F., Kim, J., Kowalczyk, E., Nasonova, O., Noilhan, J., Polcher, J., Shmakin, A., Smirnova, T., Verseghy, D., Wetzel, P., Xue, Y., Yang, Z.-L., 1998: Stand alone simulations of a boreal hydrology with land-surface schemes used in atmospheric models: PILPS phase2(d). (submitted)

Shao, Y., Anne, R.D., Henderson-Sellers, A., Irannejad, P., Thornton, P., Liang, X., Chen, T.H., Ciret, C., Desborough, C. and Barachova, O., 1994, Soil Moisture Simulation, A Report of the RICE and PILPS Workshop, GEWEX Tech. Note, IGPO Publ. Series, 14, 179 pp.

7.
Concluding Remarks

The Oregon State University (OSU) Atmospheric Boundary-Layer (ABL) model was developed to include the physics thought to be the most important for both terrestrial and marine atmospheric boundary layers, yet is designed to be sufficiently simple for application to large-scale numerical weather prediction models. As cited in earlier journal articles and Phillips Laboratory (Hanscom AFB, MA) technical reports, the two major advances in the early years of model development were a diagnostic method using the bulk Richardson number to estimate boundary-layer depth, and the replacement of the usual force-restore equations with the actual equations for heat and moisture transport in the soil. Because of the robustness of the boundary-layer and land-surface model components, model inquiries and adoption of the model or some of its concepts have continued during the contract period. The model is now being used successfully in a number of diverse applications, from operational forecast and global climate models to specific hydrometeorological case studies at more than two dozen institutions worldwide. This may be partly due to the continued cooperation between researchers at other high profile institutions, such as the National Centers for Environmental Prediction / Environmental Modeling Center (NCEP/EMC; Washington, D. C.) and the National Center for Atmospheric Research (NCAR). (See Appendix for list of model users.)

One of the most important topics continues to be the consideration of the effect of subgrid variability, both at the surface, and in the ABL. On a smaller scale, Ek and Mahrt (1998; Chapter 2) and others have shown the importance in considering fluxes in the presence of sparse canopies; this is an additional consideration (on a smaller scale) beyond 'tiling' where a NWP grid box is subdivided into more than one homogeneous subregion. Continued collaboration between OSU and Phillips Laboratory, NCEP/EMC, and other groups, and our participation in the Project for Intercomparison of Land-surface Parameterizations Schemes (PILPS) has provided a forum for further testing and improving the land-surface scheme in the OSU ABL model (e.g. those PILPS-related studies referenced in Chapter 6). The addition of a formulation to account for the stomatal control by vegetation (which affects the calculation of surface moisture flux), has also been a significant and useful improvement (e.g. adopted by NCEP/EMC for the Eta model). Accounting for the effect of vegetation on surface fluxes at all scales will remain an important area of research.

The most important subgrid variability in the ABL is the presence of cloud cover (e.g. Ek; Chapter 5), which often does not cover an entire NWP grid box, yet has a dramatic influence on the net radiation at the surface. This in turn has an important effect on surface fluxes, with feedback to ABL processes (e.g. the Cabauw case study by Ek and Holtslag; Chapter 3). Subgrid ABL cloud cover and coupling with the surface will remain to be an important research issue (e.g. the marine ABL study by Levy and Ek; Chapter 4).

Articles prepared under AFOSR Contract No. F49620-9610058

Chang, S. and M. Ek, 1996: Sensitivity study of the CAPS model land-surface scheme using the 1987 Cabauw/PILPS data set. *Phys. Chem. Earth*, 21, 205-210.

Chang, S., D. Hahn, C.-H. Yang, D. Norquist, and M. Ek, 1998: Validation study of the CAPS model land-surface scheme using the 1987 Cabauw/PILPS data set. *J. Appl. Meteorol.* (to appear).

Chen, T. H., A. Henderson-Sellers, P. C. D. Milly, A. J. Pitman, A. C. M. Beljaars, S. Chang, M. Ek, and collaborators, 1997: Cabauw experimental results from the Project for Intercomparison of Land-surface Parameterization Schemes (PILPS). *J. Climate*, 10, 1194-1215.

Ek, M., 1998: A boundary-layer cloud cover formulation based on a top-hat moisture distribution. *Bound.-Layer Meteorol.* (to be submitted)

Ek, M. and A. A. M. Holtslag, 1998: The simulation of surface fluxes and boundary-layer development at Cabauw, Netherlands. *J. Appl. Meteorol.* (to be submitted)

Ek, M. and L. Mahrt, 1998: A two-source canopy model with subcanopy mixing. *Bound.-Layer Meteorol.* (to be submitted)

Levy, G. and M. Ek, 1998: The simulated response of the marine atmospheric boundary layer in the western Pacific warm pool region to surface flux forcing. *J. Geophys. Res.* (submitted)

Liang, X., E. F. Wood, D. P. Lettenmaier, D. Lohmann, S. Chang, M. Ek, and collaborators, 1998: The Project for Intercomparison of Land-surface Parameterization Schemes (PILPS) Phase 2(c) Red-Arkansas River Basin Experiment: 2. Spatial and temporal analysis of energy fluxes. *Global and Planetary Change* (to appear).

Lohmann, D., D. P. Lettenmaier, X. Liang, E. F. Wood, S. Chang, M. Ek, and collaborators, 1998: The Project for Intercomparison of Land-surface Parameterization Schemes (PILPS) Phase 2(c) Red-Arkansas River Basin Experiment: 3. Spatial and temporal analysis of water fluxes. *Global and Planetary Change* (to appear).

Qu, W. Q., A. Henderson-Sellers, A. J. Pitman, T. H. Chen, S. Chang, M. Ek, and collaborators, 1998: Sensitivity of latent heat flux from PILPS land-surface schemes to perturbations of surface air temperature. *J. Atmos. Sci.*, **55**, 1909-1927.

Wood, E. F., D. P. Lettenmaier, X. Liang, D. Lohmann, S. Chang, M. Ek, and collaborators, 1998: The Project for Intercomparison of Land-surface Parameterization Schemes (PILPS) Phase 2(c) Red-Arkansas River Basin Experiment: 1. Experiment Description and summary intercomparisons. *Global and Planetary Change* (to appear).

Appendix

Oregon State University
Atmospheric boundary-layer model users

The following list gives users of the Oregon State University (OSU) atmospheric boundary-layer (ABL) model. The OSU ABL model was originally developed as a cooperative effort between several researchers in Atmospheric Sciences at Oregon State University and in the Atmospheric Prediction Branch at Phillips Laboratory (Hanscom AFB, MA). The most recent and active users of the model are listed, along with their specific research interests, and use of the model, either the full model (land-surface and atmospheric boundary-layer schemes coupled), or some of its components. Where known, relevant publications are cited. There have been a number of other research groups from a variety of disciplines that have obtained the model code which are also identified below, but the precise usage of the model is not currently known. This list does not include 'second generation' OSU ABL model users, that is, researchers that have obtained the model code from someone else, unless contact has been made with us. This list also does not include those research groups (about 20-30) that have obtained the OSU ABL model code for inspection purposes, but have not contacted us further with the intended use of the model.

The land-surface scheme in the OSU ABL model has been included in the Project for Intercomparison of Land-surface Parameterization Schemes (PILPS; Chen et al, 1997). In that project, the land-surface scheme from the OSU ABL model is referred to as the Coupled Atmosphere-Plant-Soil (CAPS) model/land-surface scheme.

ORIGINAL DEVELOPERS

Atmospheric Sciences
College of Oceanic and Atmospheric Sciences
Oregon State University
Corvallis, OR 97331 USA

Larry MAHRT, mahrt@ats.orst.edu
tel. 503.737.5691, fax. 503.737.2540

Michael EK, ek@ats.orst.edu
tel. 503.737.5691, fax. 503.737.2540

Atmospheric boundary-layer (ABL) simulation (including shallow ABL clouds), and interaction with the land and sea surfaces. Various 1-D case studies using field programs/GCM model output data sets to formulate, test and validate the OSU-PL land-surface/atmospheric boundary-layer (full) model. Mahrt and Ek (1983), Mahrt and Pan (1984), Mahrt et al (1984), Troen and Mahrt (1986), Chu (1986), Pan and Mahrt (1987), Ruscher (1987), Mahrt et al (1987), Ek and Mahrt (1991, 1994), Mahrt et al (1991), Kim and Mahrt (1992a,b), Mahrt et al (1994), Frech and Mahrt (1995).

Atmospheric Prediction Branch
Atmospheric Sciences Division
Phillips Laboratory (PL/GPAP)
Hanscom AFB, MA 01731-5000 USA

Sam CHANG, tel. 617.377.2954, chang@plh.af.mil
Ken YANG, tel. 617.377.3913, yang@plh.af.mil
Doug HAHN, tel. 617.377.2878, hahn@plh.af.mil
Don NORQUIST, tel. 617.377.2962, norquist@plh.af.mil

Application of the full OSU-PL model to global numerical weather prediction. Also, tests using the OSU-PL land-surface package (CAPS) to test the response to atmospheric forcing on annual time scales (PILPS). Norquist and Chang (1994), Norquist et al (1994), Chang and Ek (1995), Chen et al (1996), Chang et al (1998).

OTHER USERS

National Centers for Atmospheric Prediction
Environmental Modeling Center
National Weather Service/NOAA
W/NMC22 WWB, Room 204
Washington, D. C. 20233 USA

Hua-Lu PAN, tel. 301.763.8301, hualupan@sun1.wwb.noaa.gov
Ken MITCHELL, tel. 301.763.8161, kmitch@sun1.wwb.noaa.gov
Fei CHEN, tel. 301.763.8056, fchen@sun1.wwb.noaa.gov (now at NCAR)

Parameterization of plant/soil processes and surface fluxes for global and regional operational weather forecast modeling. Pan (1990), Chen et al (1996).

Department of Meteorology 3034
Florida State University
Tallahassee, FL 32306-3034 USA

Paul RUSCHER, tel. 904.644.6205, ruscher@met.fsu.edu
Birol KARA (Ruscher student), tel. 904.644.2752, birol@met.fsu.edu

Air-mass transformation modeling using (modified) full OSU-PL model. Educational tool for graudate students.

MIT Lincoln Laboratory
Group 43, Weather Sensing
Lexington, MA 02173-9108 USA

John L. KELLER, tel. 617.981.3995, johnk@ll.mit.edu

Site specific prediction of atmospheric boundary layer structure and stratus breakup, specifically applied to short term forecasting for San Francisco Int'l Airport (current FAA project) using boundary-layer scheme, and full OSU model.

Air Force Global Weather Central (AFGWC)
SYS (AGROMET)
MBB 39
106 Peacekeeper Dr STE 2N3
Offutt AFB, NE 68113-4039 USA

Raymond B. KIESS, tel. 402-294-3373, kiessrb@oafbhost.offutt.af.mil
Thomas KOPP, tel. 402.294.3533
Brian MOORE
James CRAMER

OSU-PL land surface package used as an worldwide operational near-real time diagnostic agrometeorological model in support of AFGWC numerical weather forecasts. Full OSU-PL model for operational cloud forecasting over land.

Royal Netherlands Meteorological Institute (KNMI)
PO BOX 201
3703 AE De Bilt
THE NETHERLANDS

A. A. M. HOLTSLAG, tel. 31.30.206.458, holtslag@knmi.nl
and colleagues

Atmospheric boundary layer (ABL) mixing, coupled land-surface/ABL interaction, application to operational regional forecast model for The Netherlands. Holtslag et al (1990), Holtslag et al (1995), Holtslag and Ek (1996), Ek and Holtslag (1998).

Environmental Science
Murdoch University
Murdoch, Western Australia, 6150
AUSTRALIA

Tom LYONS, tel. 61.9.332.2413, lyons@atmos.murdoch.edu.au
Huang XINMEI (Lyons student), tel. 61.9.360.2737, xin@essun1.csu.murdoch.edu.au

Coupled land-surface/atmospheric boundary layer modeling studies with emphasis on effects of surface heteorogeneity, and more recently, modeling studies involving cloud processes and the stable boundary layer. Huang and Lyons (1995), Huang et al (1995a,b).

NOAA Environmental Research Lab
Forecast Systems Lab
R/E/FS1
325 Broadway
Boulder, CO 80301 USA

Stan BENJAMIN, tel. 303.497.6387, benjamin@fsl.noaa.gov
Tanya SMIRNOVA, tel. 303.497.6253, smirnova@fsl.noaa.gov
John BROWN, jmbrown@mtn.fsl.noaa.gov
Zaitao PAN, pan@profsc.fsl.noaa.gov

Land-surface processes modeling as part of the Mesoscale Analysis and Prediction System (MAPS) NMC project, which provides high-frequency analyses and short-range forecasts to different mesoscale users.

Lawrence Livermore National Laboratory, L262
PO Box 808

Livermore, CA 94551 USA

Jinwon KIM, tel. 510.422.1848, kim1@llnl.gov

Long time scale (several months) land-surface surface hydrological modeling studies. Kim and Ek (1995).

Bioresource Engineering
Water Resources Engineering Team
Gilmore Hall, Oregon State University
Corvallis, OR 97331-3906 USA

Richard H. CUENCA, tel. 503.737.6307, cuencarh@pandora.bre.orst.edu

Coupled land-surface/atmospheric boundary-layer interaction, with emphasis on parameterization of plant and soil physics using the land-surface package, and the full OSU-PL model. Ek and Cuenca (1994), Cuenca et al (1996).

National Center for Atmospheric Research (NCAR)
Climate and Global Dynamics (CGD) Division
P. O. Box 3000
Boulder, CO 80307-3000 USA

Byron BOVILLE, tel. 303-497-1337, boville@ncar.ucar.edu
Joe TRIBBIA, tel. 303.497.1377, tribbia@ncar.ucar.edu
Keith AYOTTE, ayotte@ncar.ucar.edu

Atmospheric boundary layer mixing, and application to global modeling in the NCAR Community Climate Model (CCM2) using OSU-PL boundary-layer scheme. Holtslag and Moeng (1991), Holtslag and Boville (1993), Ayotte et al (1995).

Dept of Atmospheric Sciences, AK-40
University of Washington
Seattle, WA 98195 USA

Gad LEVY, tel. 206.543.4595, gad@atmos.washington.edu

Sea surface flux parameterization and the effect on marine atmospheric boundary-layer (MABL) development using modified form of the full OSU-PL model for over ocean. Currently analyzing MABL in TOGA-COARE data set. Levy and Ek (1998).

Cole MCCLANDISH (Levy student).

OSU-PL boundary-layer model code used for marine boundary-layer depth diagnosis in tropical (trade wind) regions.

Department of Civil Engineering
University of Washington
Seattle, WA 98195

Dennis LETTENMAIER

Department of Meteorology
Universtiy of Helsinki
Hallituskatu 11-13
SF 00100 Helsinki 10
FINLAND

Antti AROLA (Lettenmaier student), aarola@cc.helsinki.fi

Land-surface/atmospheric boundary-layer interaction and sensitivity studies using the full OSU-PL model, and the OSU-PL atmospheric boundary-layer mixing scheme coupled with the VIC-2L land surface scheme. VIC was developed partly at Univ. Washington (by Dennis Lettenmaier) and partly at Princeton (by Eric Wood). Application to FIFE, HAPEX-MOBILHY, and other data sets.

Water Resources Program
C-332 E-Quad
Dept. of Civil Engineering and Operations Research
Princeton University
Princeton, NJ 08544 USA

Eric WOOD
Christa PETERS-LIDARD (Wood student), tel. 609.258-4869, cpeters@earth.princeton.edu

Land-surface/atmospheric boundary-layer interaction and sensitivity studies using the full OSU-PL model, and the OSU-PL atmospheric boundary-layer mixing scheme coupled with the TOPMODEL-Based Land Atmosphere Transfer Scheme (TOPLATS), developed at Princeton (by Eric Wood and colleagues). Application to FIFE and other data sets.

Department of Atmospheric Sciences
Colorado State University
Fort Collins, CO 80523 USA

William COTTON, tel. 303-491-8593 , cotton@isis.ATMOS.ColoState.Edu
David MOCKO (Cotton student), tel. 303.491.8209, dmocko@lamar.colostate.edu

The cloud cover formulation following Ek and Mahrt (1991) and other boundary-layer cloud cover schemes were incorporated into the Regional Atmospheric Modelling System (RAMS) to test their performance against field data sets in both maritime (FIRE) and continental cloud regimes (BLX-1983). Mocko (1994), Mocko and Cotton (1995).

National Center for Atmospheric Research (NCAR)
Climate and Global Dynamics (CGD) Division
P. O. Box 3000
Boulder, CO 80307-3000 USA

William LARGE, wily@ncar.ucar.edu

Application of Troen and Mahrt (1986) atmospheric boundary layer model with nonlocal mixing to a climate model with upper oceanic mixed layer. Large et al (1994)

Department of Geophysical Sciences
Ohio University
316 Clippinger Lab
Athens, OH 45701
USA

Moid AHMAD, ahmad@ouvaxa.ucls.ohiou.edu
L. N. SASTRY (Ahmad student), ramkumar@sys2.ped.pto.ford.com

Evapotranspiration and local climate modification in an arid region (specifically southern Nevada around Pharump, west of Las Vegas), using full OSU-PL model.

Swedish Meteorological and Hydrological Institute (SMHI)
S-60176 Norrkoeping SWEDEN

Stefan GOLLVIK

OSU-PL atmospheric boundary-layer scheme modified by Holtslag and Boville (1993) for use in the HIRLAM regional weather forecast model. Gollvik et al (1995)

Department of Meteorology
Wageningen Agricultural University
Duivendaal 1-2
6701 AP Wageningen
THE NETHERLANDS

Henk A. R. de BRUIN, tel. 31.83.708.3981, Henk.deBruin@USERS.MET.WAU.NL
Cor M. J. JACOBS, Cor.Jacobs@Users.MET.WAU.NL

Interactive land-surface/atmospheric boundary-layer studies and effects of climate change using modified form of full OSU-PL model. Jacobs (1994).

OTHER USES/USERS

European Centre for Medium-Range Weather Forecasts
Shinfield Park
Reading, Berkshirt RG2 9AX ENGLAND

Anton BELJAARS, at KNMI, The Netherlands through December 1995: beljaars@knmi.nl, tel. 31.30.206.389; ECMWF thereafter, tel. 44.734.499.000.
J.-F. MAHFOUF

Modified form of Troen and Mahrt (1986) used in ECMWF boundary-layer turbulent mixing.

Dept of Atmospheric Sciences, AK-40
University of Washington
Seattle, WA 98195 USA

Tony BEESLEY, tony@nansen.apl.washington.edu

Clouds and climate study of the central Arctic using the radiative transfer and boundary-layer mixing (modified) routines from the NCAR CCM2, and a simple 1-D sea-ice model at the surface. The NCAR CCM2 boundary-layer mixing scheme is based on Troen and Mahrt (1986) and Holtslag and Boville (1993).

Alfred Wegener Institute for Polar and Marine Research
D27570 Bremerhaven
GERMANY

Christof LUPKES

Meteorological Institute
University of Hamburg
GERMANY

Heinke SCHLUNZEN

Use of OSU-PL model with some imporvements; paper submitted to Bound.-Layer Meteorol.

National Weather Service
Medford WSFO
4000 Cirrus Drive
Medford, OR 97504-4187 USA

Dennis GETTMAN, Science and Operations Officer, tel. 503.773.1067, stres@aol.com

Numerical guidance to deal with stratus and fog dissipation/formation in the valleys of western Oregon, as well as out along the coast; similar interest as John Keller, MIT Lincoln Lab.

Battelle Pacific Northwest Laboratories
P. O. Box 999
Richland, WA 99352 USA

John HUBBE, tel. el. 509-376-4491, jm_hubbe@pnl.gov
C. D. WHITEMAN

Surface fluxes and landscape heteorogenity in arid/irrigated regions (eastern Oregon/Washington) using full OSU-PL model.

Indian Institute of Tropical Meteorology
Pune 411 008 INDIA

Surendra S. PARASNIS, pmamail@tropmet.ernet.in

Tropical atmospheric boundary-layer modeling and surface energy budget studies, and comparison with the observations from a land-surface experiment in India in 1995.

Dept. of Civil and Environmental Engineering
University of Cincinnati
Cincinnati, OH 45221-0071
USA

Shafiqul ISLAM, sislam@fractals.cee.UC.EDU
Zhenglin HU (ISLAM student), zhu@fractals.cee.uc.edu

Coupling OSU-PL boundary-layer mixing scheme with the BATS land-surface scheme to study land-surface/atmosphere interactions.

Dept de Termodinamica
Universitat de Valencia
SPAIN

Ernesto LOPEZ-BAEZA, tel: 34.96.386.4300 ext. 3279, lopez@vm.ci.uv.es

Simulations using the OSU-PL land-surface package for a semi-arid region (EFETA project, Spain) related to burned and unburned landscapes, saline and non-saline soils, and irrigated and nonirrigated crops.

Escuela de Agrono'mia
Universidad de Talca
Casilla 747, Talca
CHILE

Samuel O. ORTEGA-FARIAS, sortega@maule.utalca.cl
tel. 56.71.226.055, 56.71.220.110, fax. 56.71.228.054

OSU-PL surface flux algorithm used to estimate daytime variation of evapotranspiration for agricultural crops. Ortega-Farias (1993), Ortega-Farias et al (1995).

Institute of Hydrology
Wallingford (sent code)
Oxfordshirt OX10 8BB
UNITED KINGDOM

Alistair CULF

Centro Tecnico Aeroespacial (CTA)
Instituto de Aeronautica e Espaco (IAE)
Divisao de Ciencias Atmosfericas (ACA)
Sao Jose dos Campos
CEP 12228-904 SP
BRASIL

Gilberto FISCH, tel. 0123.41.4611 ext. 330, IAEACA@fpsp.fapesp.br

Entire OSU-PL model to study energy balance for scenarious of forest and pasture using an Amazonia data-set.

Department of Agricultural Engineering
Iowa State University
Ames, Iowa 50011 USA

Michael D. MCCORCLE

Land-surface/atmosphere interaction using the 1983 AFGL soil sodel (OSU-PL land-surface scheme) coupled to a boundary layer model developed by Jan Paegle, Univ. Utah.

Ciudad Universitaria
Pabellon 2, Piso 2
Departamento de Ciencias de la Atmosfera
1428 Capital Federal
ARGENTINA

Juan Carlos TORRES, torres@cima.uba.ar

Coupled land-surface/atmosphere studies using MCCORCLE-PAEGLE soil-atmospheric model, extended to entire troposphere.

New Zealand Meteorological Service
Industrial and Environmental
Meteorology Group
30 Salamanca Rd
PO Box 722
Wellington 1
NEW ZEALAND

BELL Martin, fax. 64.9.373.7571, mjb@phyv1.auckland.ac.nz

Regional modelling of cloud development associated with surface conditions using data from a New Zealand land-atmospheres interactions experiment (OASIS-Manawatu). OSU-PL cloud scheme of interest to the OASIS project.

Australian National University
Centre for Resource and Environmental Science, Room 403
GPO Box 4 Canberra ACT 2601
AUSTRALIA

Geraldine A. CUSACK, tel. 06.249.4053, cusack@cres.anu.edu.au

Land-surface/atmospheric/hydrological study using the OSU-PL model to determine the vertical development/profiles of moisture and energy over each of the sub-catchments in the Warragamba watershed (Australia), coupled to a basic surface hydrological model to represent the rainfall, runoff, streamflow and infiltration. Associated with Lyons group in Australia.

Italian Instit. for Env. Analysis and Remote Sensing for Agric.
Centre for Research / Environmental Science
CNR-IATA
Piazzale delle Cascine n 18
50144 Firenze ITALY

Barry MASUMBA, IATACNR@IFIIDG (bitnet)

Coupled land-surface/atmospheric boundary layer modeling studies with emphasis on effects of surface heteorogeneity. Associated with Lyons group in Australia.

U.S. Geological Survey
5735 Kearny Villa Rd
Suite O
San Diego, CA 92123 USA

Michael DETTINGER, tel. 619.637.6845, mddettin@s101pcasnd.wr.usgs.gov

OSU-PL model used to simulate land-air interactions, and comparision with a more idealized theoretical model as part of his dissertation (under Michael Ghil, UCLA Dept Atm Sci).

Dept. of Atmospheric Science
P.N.U. Pusan
609 - 735 Korea

Cho BYUNG-GIL, gbcho@hyowon.pusan.ac.kr

Use of OSU-PL model to study numerical and physical parameterizations in atmospheric boundary-layer modeling, with emphasis on radiation and heat budgets.

Atmospheric Environmental Service
Toronto, CANADA

Trevor SCHOLTZ

Atmospheric boundary layer/soil modeling of chemical transport.

Centre for Atmospheric Sciences
University of Calcutta
92, A. P. C. Road
Calcutta - 700 009
INDIA

Sutapa CHAUDHURI
M. CHATTERJEE

OSU-PL model with application to monsoon/tropical meteorology.

Atmospheric Sciences Research Center
State University of New York
Albany, NY USA

Xin-Zhong LIANG

Full OSU-PL model for use in large-scale modeling.

NASA/GSFC
Code 912
Greenbelt, MD 20771 USA

Peter WETZEL, tel. 301.286.8576, wetzel@elena.gsfc.nasa.gov

Boundary-layer cloud parameterization.

National Center for Atmospheric Research (NCAR)
P. O. Box 3000
Boulder, CO 80307-3000 USA

Mitch MONCRIEFF, moncrief@ncar.ucar.edu

Deep convection studies and interest in putting the OSU-PL model into a high resolution model of convective storms.

State Climate Office
Oregon State University
Corvallis, OR 97331-2209 USA

Geoge TAYLOR, tel. 503.737.5705, taylor@ats.orst.edu

Land-surface/atmosphere interaction and local climate.

USAF
Environmental Tech. Applications Center DNO
Air Weather Service
Scott AFB, IL

David ZEHR

Low-level wind forecasting.

National Weather Service
Forecast Office
Madison, WI USA

John EISE

Aid in operational local weather forecasting.

National Weather Service
Forecast Office
Portland, OR 97213 USA

George MILLER

OSU-PL model used as '1st guess' guidance tool in local weather forecasting, possible application to fire weather.

National Weather Service
River Forecast Center
Portland, OR 97213 USA

Charles ORWIG

Seasonal assessments of soil moisture/hydrology.

Meteorological Service
Nicosia, CYPRUS

Stelios PASHIARDIS, Meteorological Officer

Regional evaporation studies.

REFERENCES

Ayotte, K. W., P. P. Sullivan, A. Andren, S. C. Doney, A. A. M. Holtslag, W. G. Large, J. C. McWilliams, C.-H. Moeng, J. Tribbia, and J. C. Wyngaard, 1995: An evaluation of neutral and convective planetary boundary layer parameterizations relative to large eddy simulations. *J. Geophys. Res.*

Chang, S., D. Hahn, C.-H. Yang, D. Norquist, and M. Ek, 1998: Validation study of the CAPS model land-surface scheme using the 1987 Cabauw/PILPS data set. *J. Appl. Meteorol.* (to appear).

Chen, F., K. Mitchell, J. Schaake, Y. Xue, H.-L. Pan, V. Koren, Q. Y. Duan, M. Ek, and A. Betts, 1996: Modeling of land surface evaporation by four schemes and comparison with FIFE observations. *J. Geophysical Research*, **101**, 7251-7268.

Chen, T. H., et. al., 1997: Cabauw Experimental Results form the Project for Intercomparison of Land-Surface Parmeterization Schemes. *J. Climate*, **10**, 1194-1215.

Chu, C.-T., 1986: Parameterization of shallow convection in the boundary layer. Master's Thesis, Atmospheric Sciences, Oregon State University, Corvallis OR 97331, USA.

Cuenca, R. H., M. Ek, and L. Mahrt, 1996: Impact of soil water property parameterization on atmospheric boundary-layer simulation. *J. Geophys. Res.*, **101**, 7269-7277.

Ek, M. and R. H. Cuenca, 1994: Variation in soil parameters: Implications for modeling surface fluxes and atmospheric boundary-layer development. *Bound.-Layer Meteorol.*, **70**, 369-383.

Ek, M. and A. A. M. Holtslag, 1998: The simulation of surface fluxes and boundary-layer development at Cabauw, Netherlands. *J. Appl. Meteorol.* (to be submitted)

Ek, M. and L. Mahrt, 1991: A model for boundary-layer cloud cover, Ann. Geophys. 9, 716-724.

Ek, M. and L. Mahrt, 1994: Daytime evolution of relative humidity at the boundary-layer top. Mon. Wea. Rev., 122, 2709-2721.

Frech, M. and L. Mahrt, 1995: A two-scale mixing formulation for the atmospheric boundary layer. Bound.-Layer Meteorol., 73, 91-104.

Gollvik, S., B. Bringfelt, V. Perov, and A. A. M. Holtslag, 1995: Experiments with nonlocal vertical diffusion in High Resolution Limited Area Modelling (HIRLAM). The HIRLAM 3 Project, Technical REport No. 18, Swedish Meteorological and Hydrological Institute (SMHI), S-601 76 Norrkoeping, Sweden.

Holtslag, A. A. M., E. I. F. de Bruijn, and H.-L. Pan, 1990: A high resolution air mass transformation model for short-range weather forecasting. Mon. Wea. Rev., 118, 1561-1575.

Holtslag, A. A. M. and B. Boville, 1993: Local versus nonlocal boundary-layer diffusion in a global climate model. *J. Climate*, **6**, 1825-1842.

Holtslag, A. A. M. and M. Ek, 1996: The simulation of surface fluxesand boundary-layer development over the pine forest in HAPEX-MOBILHY. *J. Applied Meteorol.*, **35**, 202-213.

Holtslag, A. A. M., E. van Meijgaard, and W. C. de Roy, 1995: A comparison of boundary layer diffusion schemes in unstable conditions over land. *Bound.-Layer Meteorol.*, **76**, 69-95.

Holtslag, A. A. M. and C.-H. Moeng, 1991: Eddy diffusivity and countergradient transport in the convective atmospheric boundary layer. *J. Atmos. Sci.*, **48**, 1690-1698.

Huang, Xinmei and T. J. Lyons, 1995: On the simulation of surface heat fluxes in a land surface-atmosphere model. *J. Appl. Meteorol.*, **34**, 1099-1111.

Huang, Xinmei, T. J. Lyons, R. C. G. Smith and J.M. Hacker, 1995a: Estimation of land surface parameters using satellite data. *Hydrological Processes*, **9**, 631-643.

Huang, Xinmei, T. J. Lyons and R. C. G. Smith, 1995b: The meteorological impact of replacing native perennial vegetation with annual agricultural species. *Hydrological Processes*, **9**, 645-654.

Jacobs, C. M. J., 1994: Direct impact of atmospheric CO2 enrichment on regional transpiration. PhD thesis, Wageningen Agricultural University, The Netherlands, 179 pp.

Kim, J. and M. Ek, 1994: A simulation of the surface energy budget and soil water content over the HAPEX-MOBILHY forest site. *J. Geophys. Res.*, **100**, 20845-20854.

Kim, J. and L. Mahrt, 1992: Momentum transport by gravity waves. *J. Atmos. Sci.*, **49**, 735-748.

Kim, J. W. and L. Mahrt, 1992: Simple formulation of turbulent mixing in the stable free atmosphere and nocturnal boundary layer. *Tellus*, **44a**, 381-394.

Large, W. G., J. C. McWilliams, and S. C. Doney, 1994: Oceanic vertical mixing: a review and a model with a nonlocal boundary layer parameterization. *Reviews Geophys.*, **32** (4), 363-403.

Levy, G. and M. Ek, 1998: The simulated response of the marine atmospheric boundary layer in the western Pacific warm pool region to surface flux forcing. *J. Geophys. Res.* (submitted)

Mahrt, L. and M. Ek, 1984: The influence of atmospheric stability on potential evaporation. *J. Clim. Appl. Meteor.*, **23**, 222-234.

Mahrt, L., M. Ek, J. Kim, A. A. M. Holtslag, 1991: Boundary-layer parameterization for a global spectral model. Final Report, PL-TR-91-2031. [Available from Phillips Laboratory, Hanscom AFB, Mass. 01731-5000, USA]

Mahrt, L., M. Ek, J. Sun, M. Frech, 1994: Marine boundary-layer parameterizations for large–scale models. Final Report, PL-TR-94-2128. [Available from Phillips Laboratory, Hanscom AFB, Mass. 01731-5000, USA]

Mahrt, L. and H.-L. Pan, 1984: A two-layer model of soil hydrology. *Bound.-Layer Meteorol.*, **29**, 1-20.

Mahrt, L., H.-L. Pan, P. Ruscher and C.-T. Chu, 1987: Boundary-layer parameterization for a global spectral model. Final contract report (AFGL-TR-87-0246) to Atmospheric Prediction Branch, Air Force Geophysics Laboratory, Hanscom AFB, MA, 182 pp. Oregon State University, Corvallis.

Mahrt, L., J. O. Paumier, H.-L. Pan and I. Troen, 1984: A boundary-layer parameterization for a general circulation model. Final contract report (AFGL-TR-84-0063) to Atmospheric Prediction Branch, Air Force Geophysics Laboratory, Hanscom AFB, MA, 179 pp. Oregon State University, Corvallis.

Mocko, D. M., 1994: Diagnosing boundary-layer cloudiness in a mesoscale model. Air Force Office of Scientific Research Report No. AFOSR-91-0269. (also Master's thesis, Colorado State Univ., Paper No. 553, 107 pp, W. Cotton, advisor.)

Mocko, David M. and William R. Cotton, 1995: Evaluation of fractional cloudiness parameterizations for use in a mesoscale model. *J. Atmos. Sci.*, **52**, 2884-2901. (Special JAS issue on marine boundary layer clouds with emphasis on FIRE and ASTEX.)

Norquist, D., and S. Chang, 1994: Diagnosis and correction of systematic humidity error in a global numerical weather prediction model. *Mon. Wea. Rev.*, **122**, 2442-2460.

Norquist, D., D. Hahn and S. Muench, 1994: Diagnosing cloudiness from global numerical weather prediction forecasts. Phillips Laboratory technical report, PL-TR-94-2211, July.

Ortega-Farias, S. O., 1993: A Comparative Evaluation of Residual Energy Balance, Penman, and Penman-Monteith Estimates of Daytime Variation of Evapotranspiration. Ph.D Thesis, Oregon State University, Corvallis, Oreg. 97331 USA.

Ortega-Farias, S., R. H. Cuena, and M. Ek, 1995: Daytime variation of sensible heat flux estimated by the bulk

aerodynamic method for a grass canopy. *Agric. and Forest Meteor.*, **81**, 131-143.

Pan, H.-L. and L. Mahrt, 1987: Interaction between soil hydrology and boundary layer development. Bound.-Layer Meteorol., 38, 185-202.

Ruscher, P. H., 1987: An examination of structure and parameterization of turbulence in the stably-stratified atmospheric boundary layer. Ph. D. thesis, Department of Atmospheric Sciences, Oregon State University, Corvallis, 170 pp.

Troen, I. and L. Mahrt, 1986: A simple model of the atmospheric boundary layer: Sensitivity to surface evaporation. *Bound.-Layer Meteorol.*, 37, 129-148.